SI Materials and Methods

TBK1 phosphoproteomics

Cell culture and SILAC labeling: Lung adenocarcinoma cell lines used for this study were cultured in RPMI 1640 medium (Invitrogen) supplemented with 10% FBS and 1% penicillin/streptomycin. For SILAC experiments, A549 cells were grown in medium containing "heavy" [$^{13}C_6$]-L-Lys and [$^{13}C_6$, $^{15}N_4$]-L- Arg and "light" [$^{12}C_6$]-L-Lys and [$^{12}C_6$, $^{14}N_4$]-L- Arg for 7 days. At the end of 7 days, in the "biological replicate #1," light cells were used as control (scrambled shRNA) and heavy cells were infected with lentivirus encoding sh-TBK1. In a parallel "biological replicate #2," heavy cells were used as control and light cells were infected with sh-TBK1. Forty-eight hours after infection, cell pellets were collected in ice-cold PBS, washed twice, and then suspended in 300 µL of lysis buffer (20 mM HEPES pH 8.0, 9 M urea, 1 mM sodium orthovanadate, 2.5 mM sodium pyrophosphate, 1 mM β-glycerophosphate). Using a microtip (Branson, Cell Discruptor 200), we sonicated each suspension at 15 W output with 3 bursts of 30 seconds each, followed by cooling on ice for 10 seconds between each burst. Lysates were cleared by centrifugation at 16,000 x g for 20 minutes. Protein concentrations were determined with Bradford assay.

Trypsin digestion and SCX fractionation: In both biological replicates, equal amounts of protein from heavy and light extracts were mixed. The mixture (1.664 mg) was reduced with 4.5 mM DTT at 60ºC, cooled to room temperature, and then alkylated with 10 mM iodoacetamide at room temperature in the dark. Reduced and alkylated proteins were diluted 4-fold with 20 mM HEPES buffer, pH 8.0, to a final concentration of 2 M urea and digested overnight at 37ºC with 1:40 enzyme:protein ratio sequencing grade modified trypsin (Promega, Madison, WI). The resulting peptide solution was de-salted using C18 reversed phase cartridges (Sep-Pak, Waters) and lyophilized. The dried peptides were dissolved in 5 mM aqueous ammonium acetate containing 20% acetonitrile, pH 2.9 (solvent A) for fractionation with strong cation exchange chromatography (SCX). The SCX separation was performed on a 4.6 mm x 100 mm column packed with 3 µm particle size, 300 Å pore size SCX resin (PolySulfoethylA, PolyLC). The peptides were eluted using the following gradient program: 5% B (500 mM aqueous ammonium acetate containing 20% acetonitrile, pH 3.7) for 10 minutes, 5% to 50% B from 10 to 55 minutes, 50% to 100% B from 55 to 56 minutes, 100% B from 56 to 66 minutes, followed by re-equilibration at 5% B. The flow rate was 1 mL/min, and 11 fractions were collected. Each fraction was lyophilized and re-dissolved in 0.1% TFA; peptides were extracted with C18 reversed phase cartridges (Hypersep, Thermo Scientific) prior to phosphopeptide enrichment.

Phosphopeptide enrichment: Phosphopeptides in each fraction were enriched using IMAC resin purchased from Sigma (PHOS-Select™ Iron Affinity Gel). Briefly, the tryptic peptides from each SCX fraction were re-dissolved in IMAC binding buffer (1% aqueous acetic acid and 30% acetonitrile (ACN). IMAC resin (20 µL slurry/mg of protein) was washed twice with binding buffer. The phosphopeptides were incubated with the IMAC resin for 30 minutes at room temperature, with gentle agitation every 5 minutes. After incubation, the IMAC resin was washed twice with *buffer 1* (0.1% acetic acid, 100 mM NaCl, pH 3.0), followed by 2 washes with *buffer 2* (30% acetonitrile, 0.1% acetic acid, pH 3.0) and 1 wash with deionized H_2O. The phosphopeptides were eluted with 20% aqueous acetonitrile containing 200 mM ammonium hydroxide and concentrated by vacuum centrifugation. Concentrated peptides were diluted with 15 µL of 2% aqueous acetonitrile with 0.1 % formic acid for LC-MS/MS analysis.

LC-MS/MS analysis: A nanoflow liquid chromatograph (U3000, Dionex, Sunnyvale, CA) coupled to an electrospray hybrid ion trap mass spectrometer (LTQ-Orbitrap, Thermo, San Jose, CA) was used for tandem mass spectrometry peptide sequencing experiments. The sample was first loaded onto a C18 reversed-phase pre-column (5 mm x 300 µm ID packed with 5 µm resin with 100 Å pore size) and washed for 8 minutes with aqueous 2% acetonitrile with 0.04% trifluoroacetic acid. The trapped peptides were eluted onto the C18 reversed phase analytical column (75 µm ID x 15 cm, C18-Pepmap 100; Dionex, Sunnyvale, CA). The following 120-minute gradient program was used with a 300 nL/min flow rate: 95% solvent A (2% acetonitrile with 0.1% formic acid) for 8 minutes, solvent B (90% acetonitrile with 0.1% formic acid) ramped from 5% to 50% over 90 minutes, and then solvent B from 50% to 90% B in 7 minutes and held at 90% for 5 minutes, followed by re-equilibration for 10 minutes. The MS scans were performed in Orbitrap (from *m/z* 450-1600) at high mass resolution (60,000 at *m/z* 400*,* AGC target 1,000,000 and maximum ion injection time 100 ms) to obtain accurate peptide mass measurement. MS/MS scans were performed in the linear ion trap (AGC target 30,000 and maximum ion injection time 100 ms). Five tandem mass spectra were collected per survey scan for charge states 1 to 4 in a data-dependent manner with exclusion for 60 seconds. Each sample was analyzed in duplicate.

Data analysis: The mass spectrometry data were analyzed using MaxQuant version 1.1.1.25 (http://www.maxquant.org). For the search parameters, double labeling with Lys-6 and Arg-10 was selected, allowing a maximum of 3 labeled amino acids (Lys and Arg) per peptide. Enzyme specificity was set to full trypsin digestion, allowing up to 2 missed cleavages. Carbamidomethylation of cysteine was set as a fixed modification; oxidation of methionine, N-terminal protein acetylation, phosphorylation of serine, threonine, and tyrosine were included as variable modifications. “First

search ppm" for the peptide mass tolerance was set to 20 ppm, and fragment ion tolerance was set to 0.6 Da. Protein and peptide false discovery rates were set to 0.01, and minimum peptide length was set to 6 amino acids. MS/MS data were searched against the IPI human database combined with common contaminants and concatenated with the reversed versions of all sequences using the Andromeda search engine integrated into MaxQuant.

Mascot searches were also performed against human entries in the Uni-Prot database to assign peptide sequences and identify their proteins of origin in order to verify the results from Andromeda. Precursor ion mass tolerance was set to 1.08 Da; fragment ion mass tolerance was set to 0.8 Da. Enzyme specificity was set to trypsin, and as many as two missed cleavages were allowed. Dynamic modifications included carbamidomethylation of cysteine, and oxidation of methionine, as well as phosphorylation of serine, threonine, and tyrosine, heavy lysine and heavy arginine. Database search results were summarized in Scaffold 3.0 (www.proteomesoftware.com).

MaxQuant output in the 'Phospho (STY)Sites.txt' files were further post-processed and phosphopeptide observations from the two biological replicates were merged together. MaxQuant can output multiple rows for a given modified peptide, which presents a challenge for merging data from different biological replicates. Specifically, which observations can be appropriately matched across biological replicates? Multiple MaxQuant rows can be produced for a variety of reasons, such as: multiple observed phosphosites per peptide, multiple potential phosphosites with individual probabilities that yield different potential phosphosequences, and multiple proteins containing the peptide. Thus, phosphopeptide observations between biological replicates should be matched together only when their attributes can be completely matched to each other using the criteria discussed in the following paragraphs.

First, entries in the 'Modified Sequence' column were reannotated to report the phosphorylation site indicated in the 'Position' column, which describes the location of the chosen phosphosite within the peptide sequence. For peptides with multiple potential phosphosites, the given modified sequence may be different from that indicated by the 'Position' column. In these cases, the p(STY) in the modified sequence within the first reported combination of potential sites remains unchanged for all other reported combinations, even when the reported phosphorylated amino acid is different. Therefore, the reannotated p(STY) is reported in a new 'Inferred Modified Sequence' column, using the given 'Modified Sequence,' 'Phospho (STY) Probabilities,' and single phosphosite 'Position' of interest for that row. If the original modified sequence listed in the MaxQuant output did not contain the reported phosphosite position, one of the existing p(STY) was relocated to the reported position.

The phosphosite to be relocated was chosen as having the lowest phosphosite probability, using the most C-terminal site in case of ties to be consistent with the observed pattern of modified sequences reported by MaxQuant.

Next, a site probability ranking, 'Phospho (STY) Probability Order,' was constructed using the corrected inferred modified sequence, so that peptides exhibiting similar phosphosite probabilities could be identified. Phosphosite probabilities were floored to an empirical minimum threshold of 0.05 and sorted from highest to lowest, with sites present in the inferred modified sequence ordered before potential sites not present in the inferred modified sequence. For each of the N observed phosphosites, the delta probability was calculated between it and the next ranked site. Sites differing by greater than 0.3333 in probability were listed with a ">>" separator between them. Sites differing by less than or equal to 0.05 were treated as equal and listed with a comma separating them. Remaining sites that differed by between 0.05 and 0.3333 in probability were listed with a single ">" between them. The N_{+1}^{th} site was then interrogated, listing a final "n" using the same rules for separator selection. Thus, the hypothetical phosphopeptide 'pYATpS' with probabilities 'Y(0.47)AT(0.52)S(1)' would result in a probability ranking of '4>>1,n', while the same phosphopeptide with probabilities 'Y(0.75)AT(0.25)S(1)' would yield a probability ranking of '4>1>>n'.

For each phosphopeptide, unique identifiers were then generated by combining the 'Inferred Modified Sequence,' 'Charge,' 'Number of Phospho (STY),' 'Position,' 'Phospho (STY) Probability Order,' 'Sequence Window,' 'Proteins,' and 'Ratio Present Flag.' The ratio present flag was set to "1" if a heavy/light (H/L) ratio was reported for the phosphopeptide and to "0" if no ratio was present (due to only observing a light or a heavy-labeled peptide), in order to prevent matching observations with ratios to those without. Phosphopeptides with 'PEP' scores > 0.5 and 'Mass Error' > 5 ppm were discarded. Biological replicates were then merged together using these generated unique identifiers, listing combinations of all vs. all rows for unique identifiers that resulted in multiple input data rows per identifier. H/L ratios were read from the 'Ratio H/L Normalized' columns, and the inverse of the ratios was used for the light-labeled experiment, to account for the L/H label swap.

GeneGO Metacore pathway analysis: For each data point in the merged dataset containing both biological replicates, a geometric mean of the two replicate ratios (shTBK1/control) was calculated, and data points with ratios < 1.5-fold were discarded. Data points exhibiting opposite fold-change directionality between replicates were also discarded. Additionally, the average and standard deviation of log2 ratios was calculated within each biological replicate, and data points with an |average Z-score| < 1 were discarded as noisy. GeneIDs, symbols, aliases, and other annotations

were assigned to each peptide based on their listed IPI and Uniprot accessions, using assembled IPI/Uniprot -> NCBI -> GeneID -> annotation mapping tables. Genes from the resulting filtered list (TBK1-regulated phosphoproteins), together with their orthologous genes from mouse and rat, were analyzed with GeneGo Metacore to identify all direct and nearby connecting literature interactions (1, 2). These interactions were exported and combined with ratio data, then reduced to a set of self-consistent interactions that agree with the observed ratios (such as decreased inhibitor levels leading to increased expression of the target gene). Genes with multiple phosphopeptide data points and observed directions of change used majority voting to determine consensus direction of change, with ties resulting in a classification of unchanged/uncertain. The results were visualized in Cytoscape. The original file can be found in Dataset S3.

Motif-x: TBK1-regulated phosphopeptides (>1.5-fold, >1 Z-score) were subjected to Motif-x (http://motif-x.med.harvard.edu/). Parameters were as follows: significance of 0.000001, occurrence of 10, and width of phosphopeptides of 13. The IPI Human FASTA Database was used as background data.

Lentivirus production and knockdown: Lentivirus was produced using ViraPower^{TM} Lentiviral Expression System (Invitrogen) according to the manufacturer's instructions. Briefly, 293FT cells were transfected with viral vectors (pLP1, pLP2, VSVG) and vectors encoding shRNAs using the calcium phosphate method. All shRNA lentiviral vectors were purchased from Open Biosystems, and the TRC identification numbers for individual shRNA are described in table S2. Viral supernatants were collected 48 and 72 hours after transfection and pooled after removing cell debris by centrifugation at 1500 rpm for 5 min, then stored at -80ºC until virus infection. The target cells were infected in the presence of 6 μg/mL polybrene for 24 hours, and then viral medium was replaced with fresh growth medium containing 2 μg/mL puromycin.

Immunoblotting: Cells were washed with ice-cold PBS and whole cell extracts (WCE) were prepared using lysis buffer (0.5% NP-40, 50 mM Tris-Cl pH 8.0, 150 mM NaCl, 1 mM EDTA) supplemented with protease inhibitor (Roche) and phosphatase inhibitor cocktail (Sigma-Aldrich). WCEs were resolved on SDS-PAGE and transferred to nitrocellulose membrane. The membrane was blocked in 5% skim milk/PBST, and then incubated overnight in primary antibodies at 4ºC. Bound antibodies were visualized by HRP-conjugated secondary antibodies and SuperSignal West Pico Chemiluminescent Substrate (Thermo Scientific).

Antibodies and reagents: Anti-TBK1, pTBK1 (Ser172), PARP, AKT, pAKT (Ser473, Thr308), ERK, pERK (Thr202/Tyr204), EGFR, pEGFR (Tyr1068), Met, pMet (Tyr1234/Tyr1235), pS6K (Thr421/Ser424), PLK1, pPLK1 (Thr210) antibodies were purchased from Cell Signaling Technology. Anti-pEGFR (Tyr1197), KRAS, β-actin, MTDH and pMTDH (Ser568) antibodies were purchased from Santa Cruz Biotechnology, Calbiochem, Sigma-Aldrich, Invitrogen, and Abcam, respectively.

Cell viability assay: Cell viability assays were performed according to the manufacturer's recommendations of CellTiter-Glo Luminescent Cell Viability Assay (Promega). Results are representative of at least two independent experiments (triplicates) with similar results.

Luciferase assay: Cells were plated on 24-well plates and then transfected with indicated reporter gene constructs with Renilla luciferase construct. Luciferase assays were performed using Dual Glo luciferase assay system (Promega) 48 hrs after transfection according to the manufacturer's protocol.

Real-time qPCR: Total RNA was prepared using the RNeasy Mini Kit (Qiagen). To obtain cDNA, 500 ng of each RNA sample was reverse transcribed using QuantiTect Reverse Transcription Kit (Qiagen). mRNA level of human IL-8 and CXCL10 was analyzed by real-time PCR using SYBR green master mix and 7900HT Fast Real Time PCR system (Applied Biosystems). Samples were normalized to the signal generated from glyceraldehyde-3-phosphate dehydrogenase (GAPDH).

Generation of stable cell lines expressing constitutively active (CA) IKKβ or IRF3: A549 cells stably expressing constitutively active (CA) IKKβ (S177/181D) or IRF3 (S396D) were generated as described previously (3, 4). Briefly, retroviruses were produced by transfecting 293T cells with retroviral vector for the mutant genes and pCL-Eco packaging plasmid. A549 cells were infected with retroviruses encoding the mutant proteins or empty vector (MIG vector), then GFP positive cell were sorted using FACS. MIG vector contains an internal ribosome entry site GFP cassette.

EMSA: Nuclear extracts were prepared from hypotonic cytosol extraction buffer (10 mM HEPES pH 7.9, 10 mM KCl, 0.1 mM EDTA, 0.3% NP-40) followed by hypertonic nuclear extraction buffer (20 mM HEPES pH 7.9, 0.4 M NaCl, 1 mM EDTA, 25% glycerol) both supplemented with protease inhibitors. ^{32}P-labeled NF-κB oligonucleotides were used for generating radiolabeled probe. Nuclear extracts were incubated with radiolabeled probe (10^5 CPU/rxn, 5% glycerol, 0.5 mM EDTA, 1 mM DTT, 50 mM NaCl, 10 mM Tris-HCl (pH 7.6), 1 µg of poly(dI-dC) (GE Healthcare), and 4 µg of bovine serum albumin in a final volume of 20 µL for 20 minutes, and subjected to electrophoresis on a 4% (w/v) polyacrylamide gel.

Cell cycle synchoronization: For double-thymidine-block, A549 cells were exposed to thymidine (2 mM) for 18 hours, washed with PBS twice, and then released to fresh media for 8 hours. Cells were grown again in thymidine-containing media for 12 hours and then washed and released from late G1 arrest. For mitotic arrest experiments, cells were exposed to nocodazole (50 ng/mL) for 18 hours, and then whole cell extracts were harvested.

TBK1 *in vitro* kinase assay: For substrate preparation, 293FT cells were transfected with pRcCMV myc-PLK1 K82R (Addgene) or pcDNA3.1-MTDH-HA (gift from Dr. Paul Fisher at Virginia Commonwealth University) plasmids, then Immunoprecipitation was performed using anti-Myc antibody (Santa Cruz Biotechnology) and HA agarose bead (Sigma), respectively. Immunopurified MTDH-HA was incubated with 40 units of λ protein phosphatase (New England BioLabs) for 30 minutes, 30ºC, and then washed with lysis buffer for 3 times and kinase buffer for 1 time. The purified substrates were incubated with recombinant TBK1 (420 ng, Life Technologies) or vehicle control in 1x kinase buffer (20 mM HEPES, 20 mM β-glycerophosphate, 100 μM Na_3VO_4, 10 mM $MgCl_2$, 50 mM NaCl, 1 mM DTT, 50 μM ATP) for 30 min, 30ºC. Phosphorylation of PLK1 and MTDH was analyzed by Western blotting using anti-pMTDH (Ser568) and anti-pPLK1 (Thr210) antibodies, respectively. GST-IRF3 recombinant protein was used as a positive control.

Analysis of MTDH expression and lung cancer patients survival using the Director's challenge dataset: Survival was calculated on the RMA-normalized (Affymetrix Power Tools) non-DFCI subset of the Director's Challenge dataset (361 samples), using the top and bottom quartiles of the MTDH 212250_at probeset expression. The Kaplan-Meier survival estimate and log-rank test were calculated and plotted using the R statistical software package.

References

1. Mouse Genome Informatics (MGI) Web, The Jackson Laboratory, Bar Harbor, Maine. World Wide Web (URL: http://www.informatics.jax.org).
2. Bult CJ, Richardson JE, Blake JA, Kadin JA, Ringwald M, Eppig JT, the Mouse Genome Database Group. (2000) Mouse genome informatics in a new age of biological inquiry. *Proceedings of the IEEE International Symposium on Bio-Informatics and Biomedical Engineering*: 29-32.
3. Zheng Y, Vig M, Lyons J, Van Parijs L, Beg AA (2003) Combined deficiency of p50 and cRel in CD4+ T cells reveals an essential requirement for nuclear factor kappaB in regulating mature T cell survival and in vivo function. *J Exp Med* 197(7):861-874.

4. Wang J*, et al.* (2010) NF-kappa B RelA subunit is crucial for early IFN-beta expression and resistance to RNA virus replication. *J Immunol* 185(3):1720-1729.

Figure Legends for Supplementary Figures

Fig. S1. Decreased cell viability after loss of TBK1. H23 and A549 cells were infected with lentiviruses encoding control shRNA (scrambled shRNA) or 2 different hairpins targeting TBK1 (shTBK1 #1, #4). Left panel: Cell viability was examined by CellTiter-Glo luminescent cell viability assay (Promega) 6 days after lentivirus infection. Triplicate experiments ± 1StdErr. Right panel: PARP cleavage induced by TBK1 loss in A549 cells. Whole cell extracts were prepared 3 days after lentivirus infection.

Fig. S2. Immunoblotting showing ectopic expression of constitutive active (CA) IκB kinase-β (IKKβ, S177/181D) and IRF3 (S396D). NS: Non-specific.

Fig. S3. Increased IL-8 mRNA, NF-κB-dependent reporter gene (NF-κB-Luc) expression in A549 cells expressing CA-IKKβ, and CXCL10 mRNA, IFN promoter (IFN-β-Luc) expression in A549 cells expressing CA-IRF3 measured by qRT-PCR and reporter gene assay, respectively.

Fig. S4. Effect of TBK1 knockdown on basal NF-κB-DNA binding measured by EMSA. Nuclear extracts were harvested 3 days after lentivirus infection. TNF was used as a positive control.

Fig. S5. Time course of induction of PARP cleavage and reduction of TBK1 expression after shTBK1 lentivirus infection.

Fig. S6. Venn diagram showing the number of phosphopeptides and phosphoproteins identified from the TBK1 phosphoproteomics experiment.

Fig. S7. Validation selected TBK1-regulated phosphopeptides by immunoblotting. Whole cell extracts were harvested 2 days after lentivirus infection.

Fig. S8. MS, MS/MS spectra, and EICs for selected TBK1-regulated phosphopeptides.

Fig. S9. Representative phospho-motifs enriched in up- and down-regulated phosphopeptides after loss of TBK1 using Motif-x. Motifs with significance of $P<10^{-6}$ are shown.

Fig. S10. Cell viability assay after pharmacological inhibition of PLK1 (BI6727 and BI2536, 0.5 μM) or TBK1 knockdown in 9 NSCLC cell lines. Cell viability was examined 3 days after drug treatment or 6

days after lentivirus infection utilizing Cell-Titer Glo assay kit (Promega). Remaining cell viabilities compared to control (DMSO and scrambled shRNA for PLK1 inhibitors and TBK1 knockdown, respectively) are shown. Duplicate (PLK1 inhibitors) and triplicate experiments (TBK1 knockdown) ± 1 StdErr.

Fig. S11. Survival in lung adenocarcinoma patients with high levels of MTDH tumor expression (red) is significantly worse than in those expressing low levels (blue).

Fig S12. TBK1 *in vitro* kinase assay using MTDH as substrate. Lambda protein phosphatase (λPP) was treated to immunopurified MTDH and then washed off before recombinant TBK1 was added. The specificity of anti-pMTDH antibody (Ser568) was validated by lack of signal from MTDH S568A mutant protein, and activity of recombinant TBK1 was validated by kinase assay using GST-IRF3 as substrate.

Fig. S13. Decreased cell viability and PARP cleavage after loss of MTDH. H23 and A549 cells were infected with lentiviruses encoding control shRNA (scrambled shRNA) or 2 different hairpins targeting MTDH (shMTDH #4, #5). Left panel: Cell viability was examined 6 days after lentivirus infection. Triplicate experiments ± 1StdErr. Right panel: PARP and MTDH immunoblotting was performed using whole cell extracts harvested 4 days (H23) and 6 days (A549) after lentivirus infection.

Fig. S14. Confirmation of knockdown and PARP cleavage after knockdown of genes indicated. Two representative cell lines (H23, sensitive to knockdown of 3 genes; and H1437, resistant to knockdown of 3 genes) were selected for immunoblotting. Whole cell extracts were harvested 4 days after lentivirus infection.

Fig. S15. Cell viability assay after TBK1, MTDH, and KRAS knockdown in 14 NSCLC cell lines. Cell viability was examined 6 days after lentivirus infection utilizing Cell-Titer Glo assay kit (Promega). Triplicate experiments ± 1StdErr.

Fig. S16. Analysis of linear correlation of relative cell viability after TBK1 and KRAS knockdown.

Fig. S17. Analysis of linear correlation of relative cell viability after MTDH and KRAS knockdown.

Fig. S18. Immunoblotting showing TBK1 knockdown in SILAC-labeled phosphoproteomics sample.

Figure S1

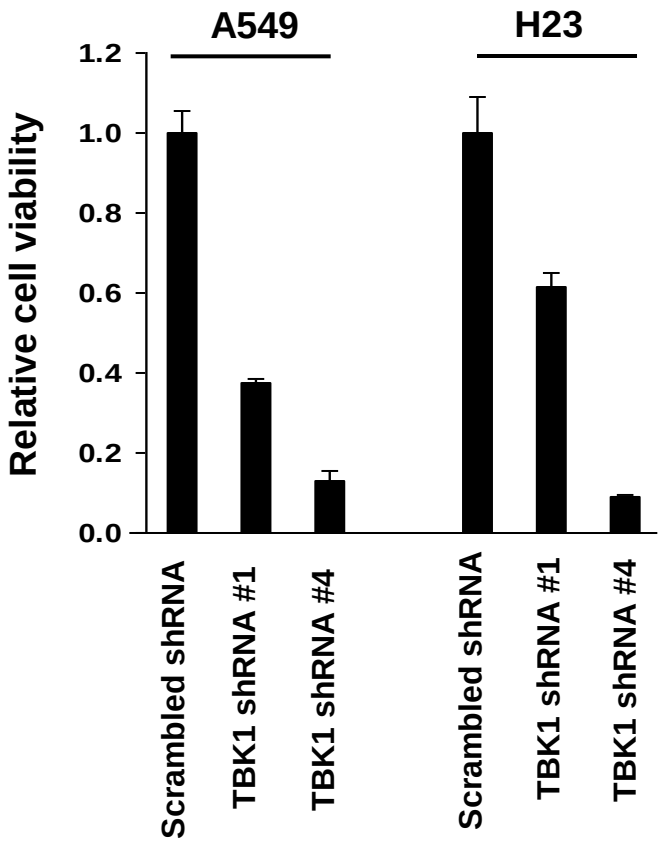
A549
H23
Relative cell viability
1.2
1.0
0.8
0.6
0.4
0.2
0.0
Scrambled shRNA
TBK1 shRNA #1
TBK1 shRNA #4
Scrambled shRNA
TBK1 shRNA #1
TBK1 shRNA #4

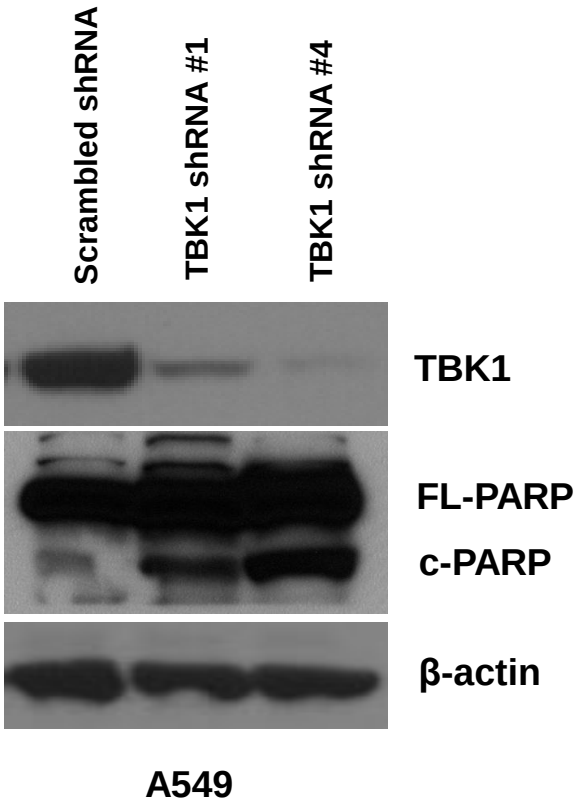
Scrambled shRNA
TBK1 shRNA #1
TBK1 shRNA #4
TBK1
FL-PARP
c-PARP
β-actin
A549

Figure S2

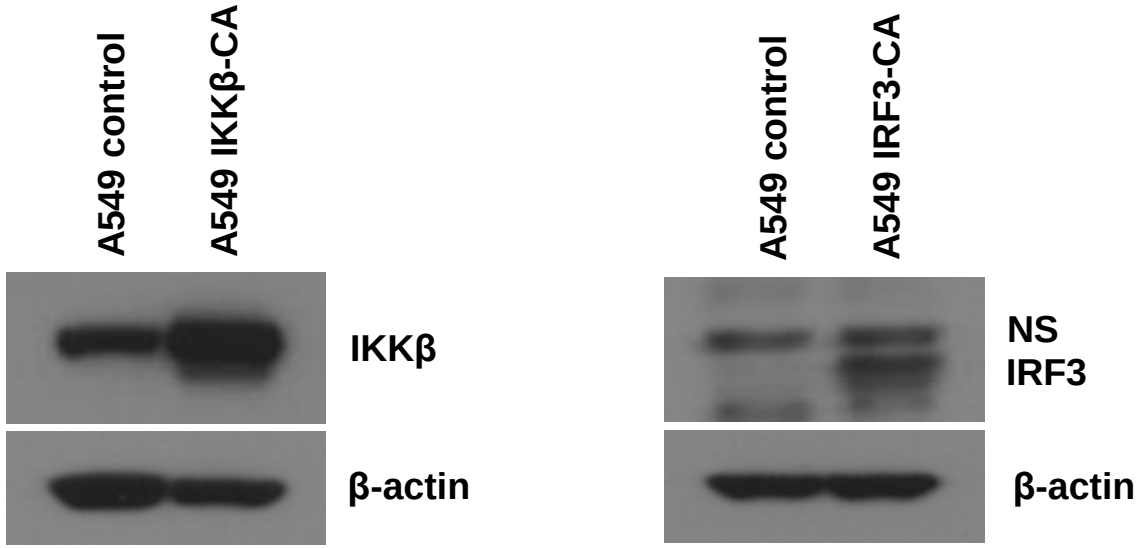
A549 control
A549 IKKβ-CA
IKKβ
β-actin
A549 control
A549 IRF3-CA
NS
IRF3
β-actin

Figure S3

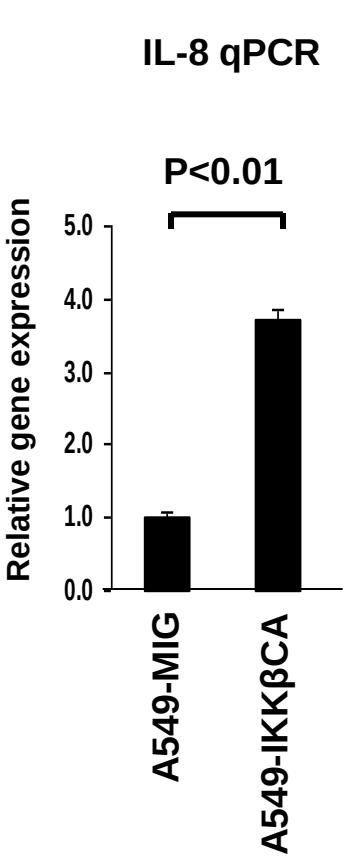
IL-8 qPCR
P<0.01
Relative gene expression
5.0
4.0
3.0
2.0
1.0
0.0
A549-MIG
A549-IKKβCA

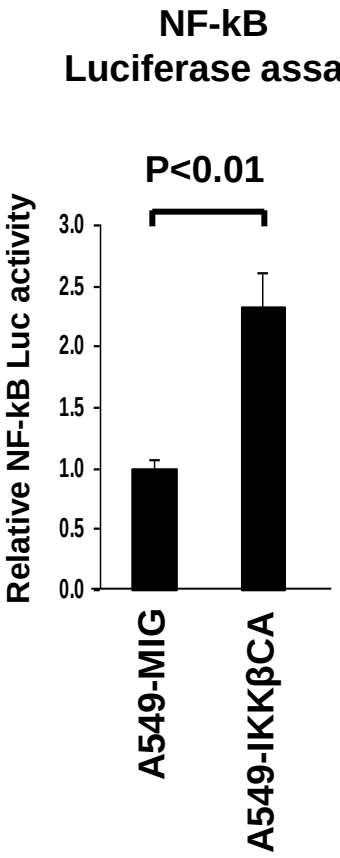
NF-kB
Luciferase assay
P<0.01
Relative NF-kB Luc activity
3.0
2.5
2.0
1.5
1.0
0.5
0.0
A549-MIG
A549-IKKβCA

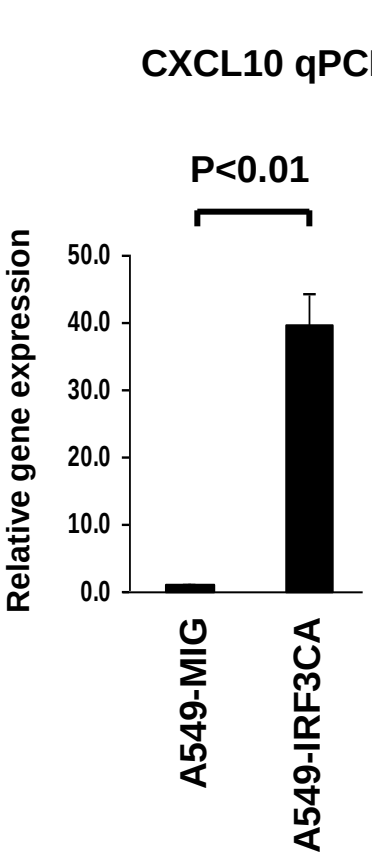
CXCL10 qPCR
P<0.01
Relative gene expression
50.0
40.0
30.0
20.0
10.0
0.0
A549-MIG
A549-IRF3CA

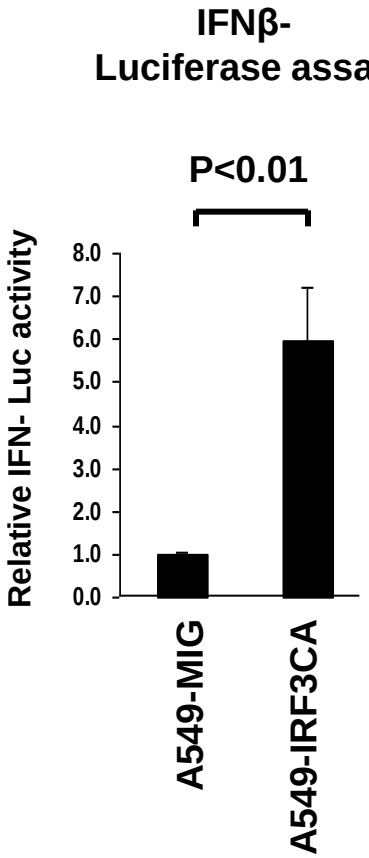
IFNβ-
Luciferase assay
P<0.01
Relative IFN- Luc activity
8.0
7.0
6.0
5.0
4.0
3.0
2.0
1.0
0.0
A549-MIG
A549-IRF3CA

Figure S4

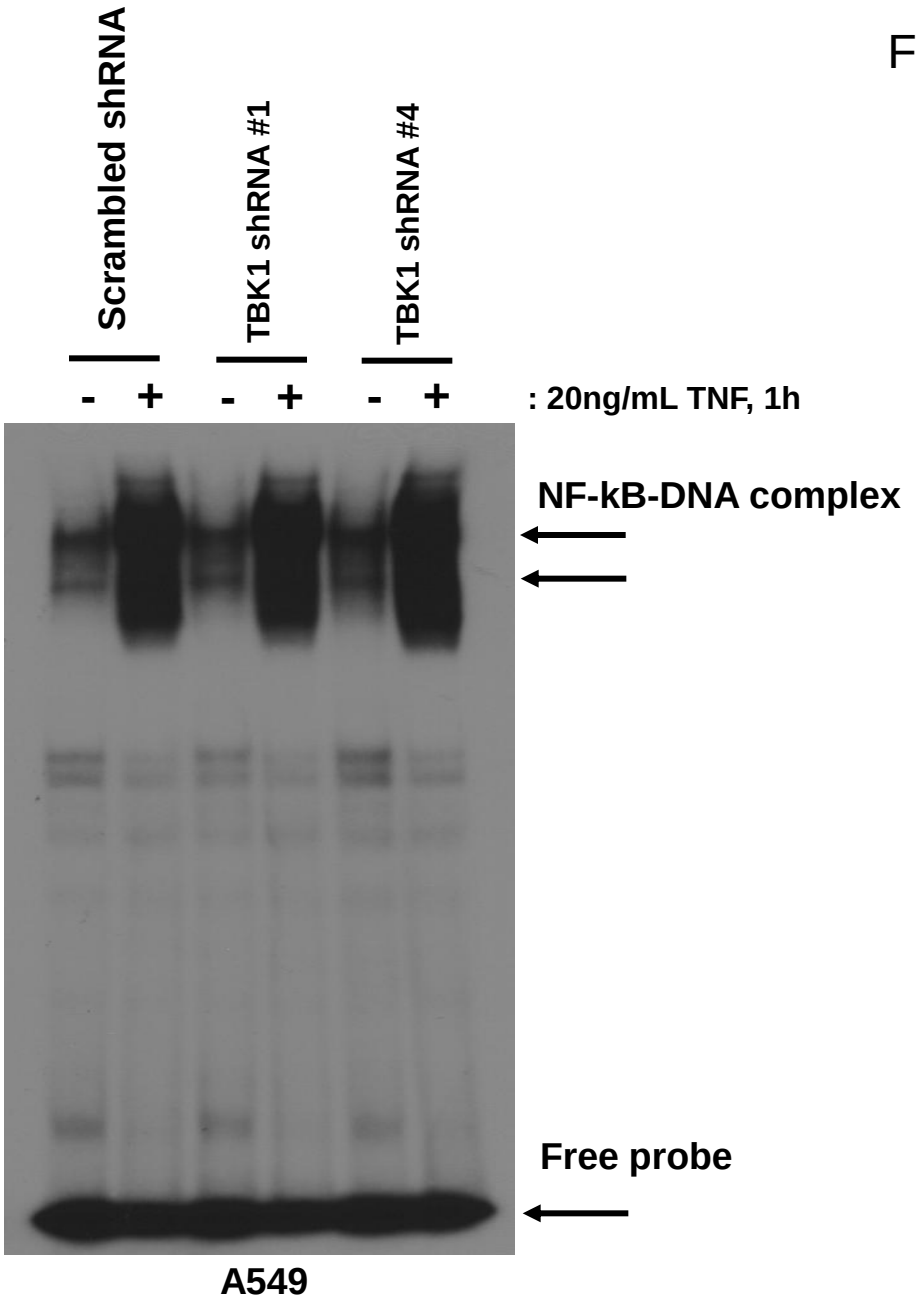
Scrambled shRNA
TBK1 shRNA #1
TBK1 shRNA #4
- + - + - +
: 20ng/mL TNF, 1h
NF-kB-DNA complex
Free probe
A549

Figure S5

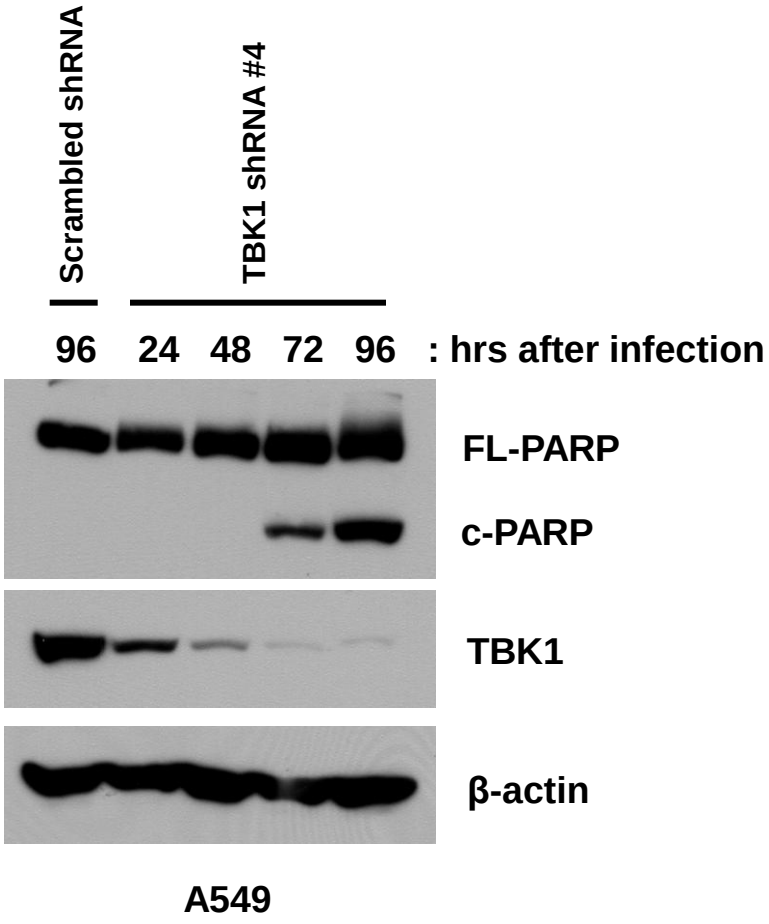
Scrambled shRNA
TBK1 shRNA #4
96
24
48
72
96
: hrs after infection
FL-PARP
c-PARP
TBK1
β-actin
A549

Figure S6

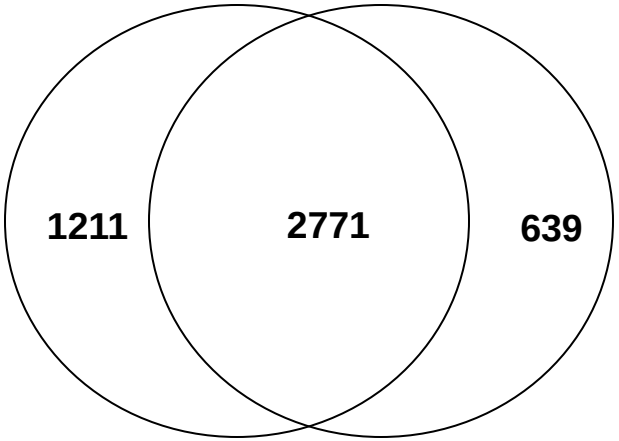

Light:control_ Heavy:shTBK1 n=3982

Light:shTBK1_ Heavy:control n=3410

4621 non-redundant phosphopeptides

Mass Error < 5ppm

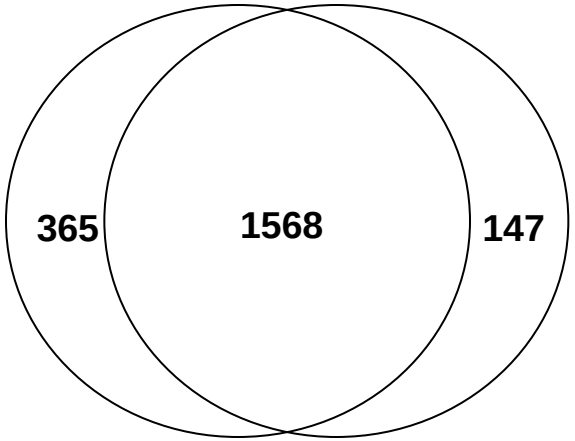

Light:control_ Heavy:shTBK1 n=1933

Light:shTBK1_ Heavy:control n=1715

2080 non-redundant phosphoproteins

Figure S7

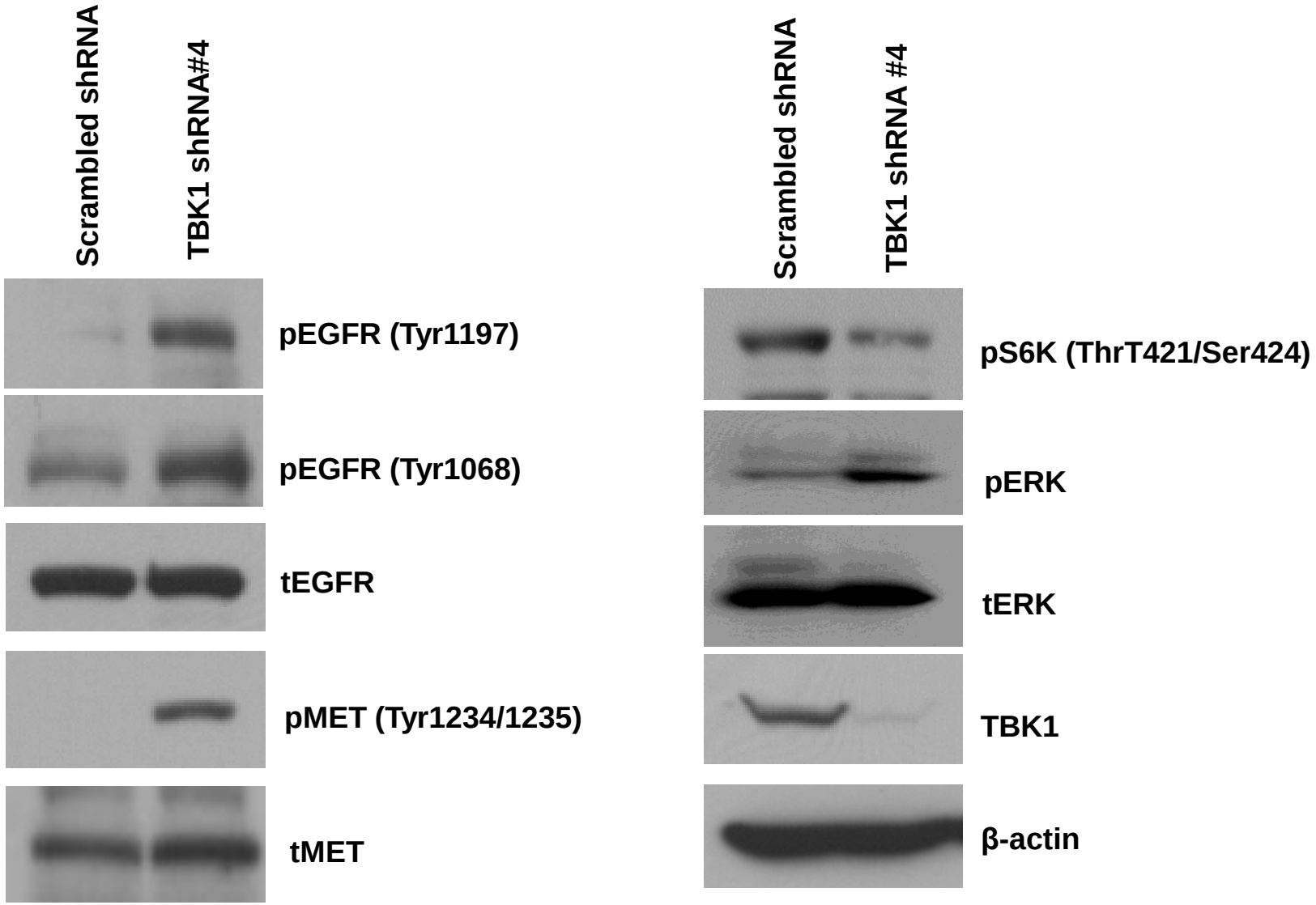
Scrambled shRNA
TBK1 shRNA#4
pEGFR (Tyr1197)
pEGFR (Tyr1068)
tEGFR
pMET (Tyr1234/1235)
tMET
Scrambled shRNA
TBK1 shRNA #4
pS6K (ThrT421/Ser424)
pERK
tERK
TBK1
β-actin

Figure S8

A. MET pY1234-Light:Control, Heavy:shTBK1

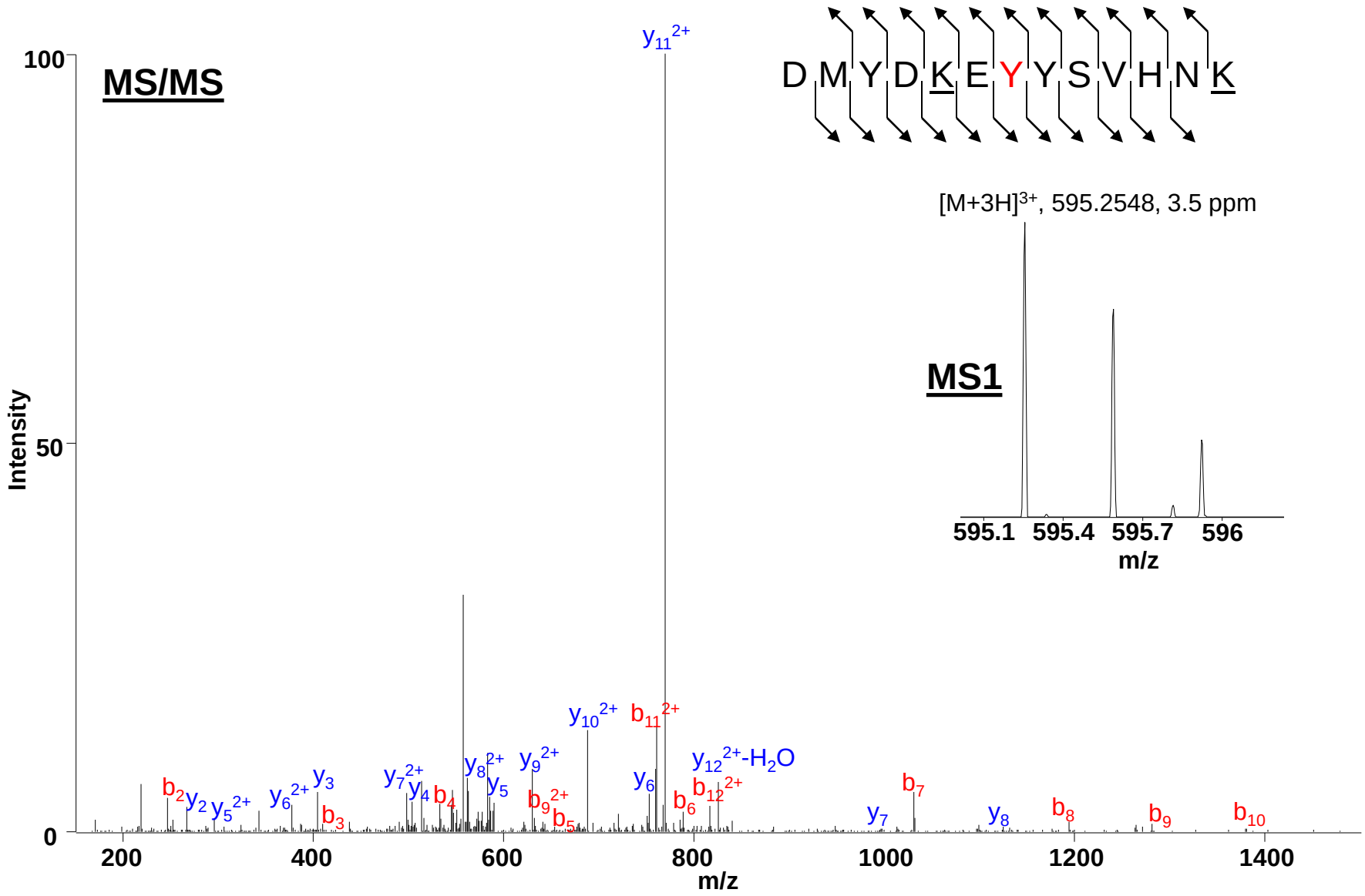

Figure S8

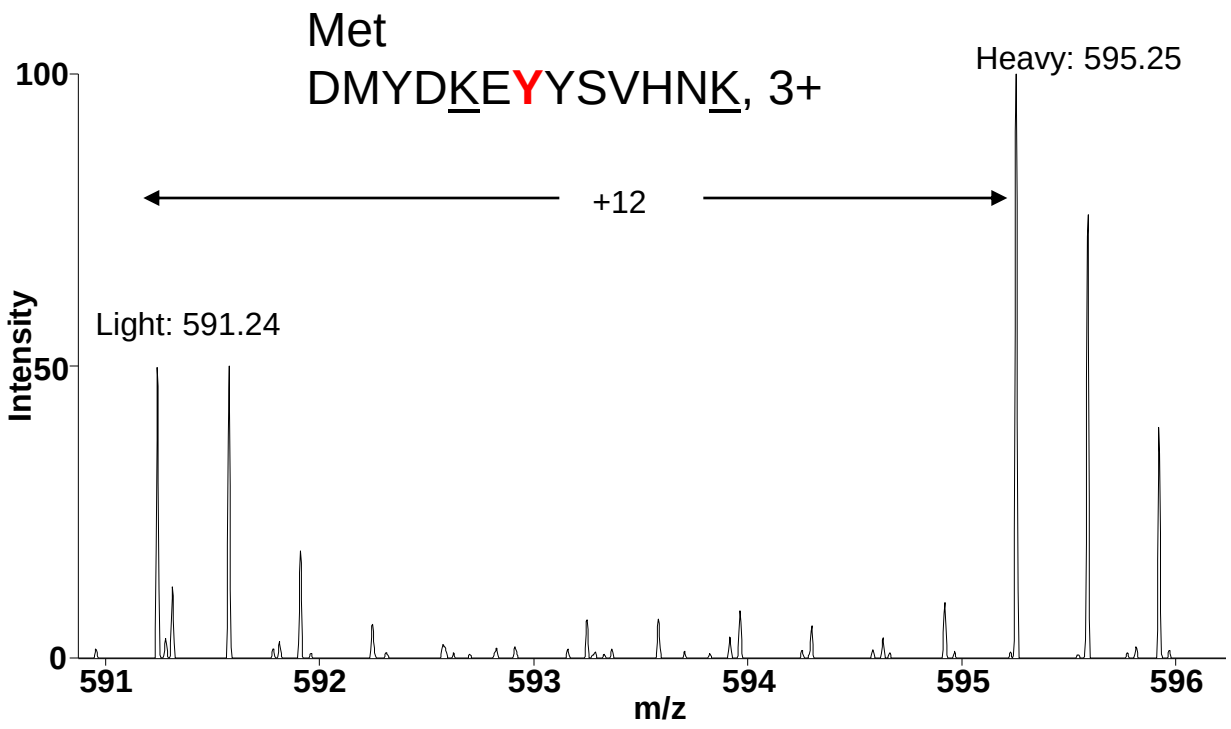

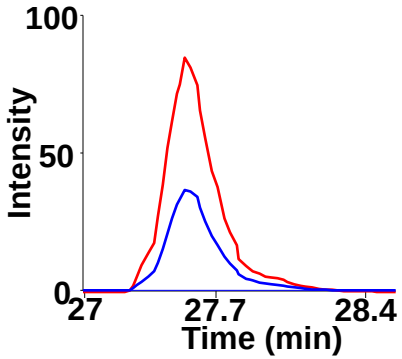

Heavy
Area: 4755389
Intensity: 255780

Light
Area: 2049496
Intensity: 110211

B. EGFR pY1172 - Light:Control, Heavy:shTBK1

Figure S8

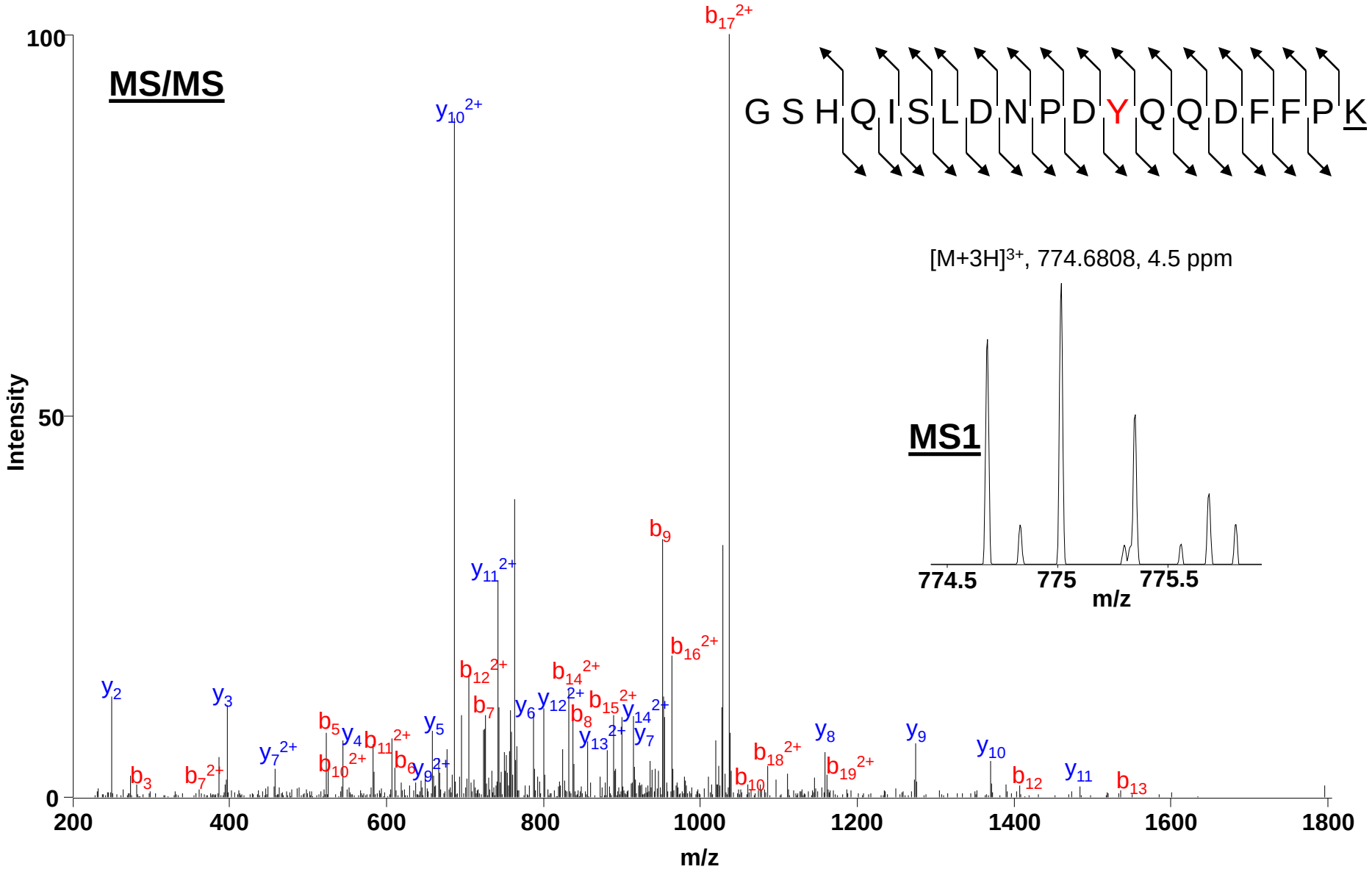

Figure S8

EGFR
GSHQISLDNPDYQQDFFPK, 3+

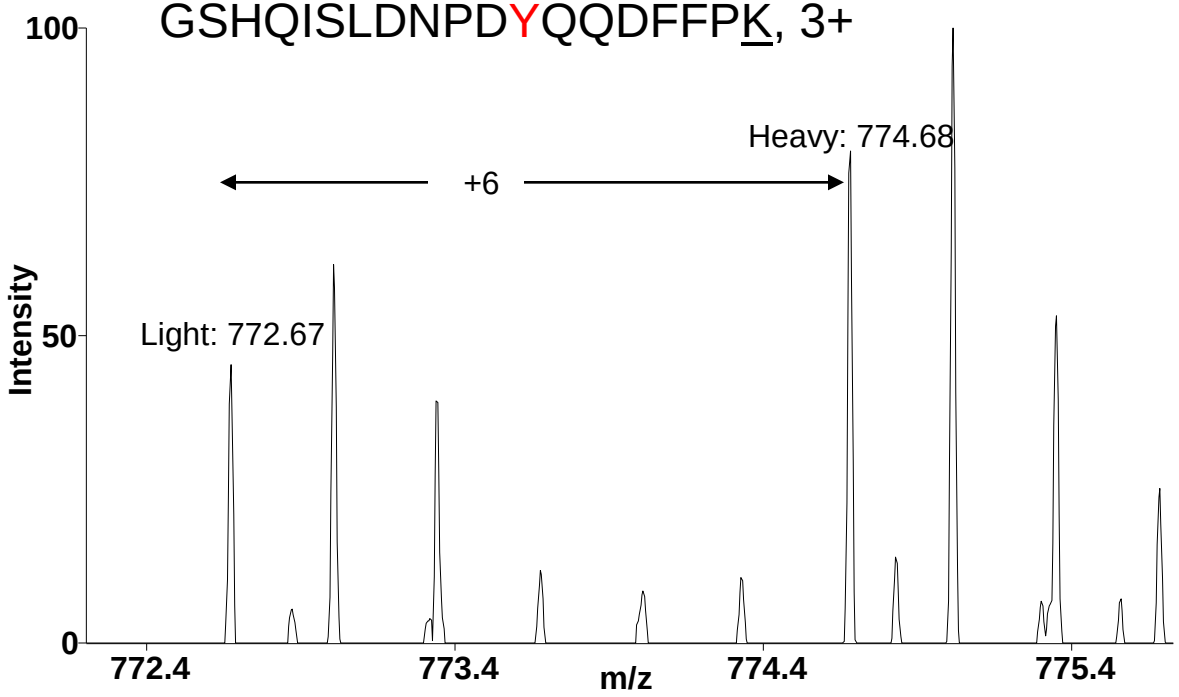

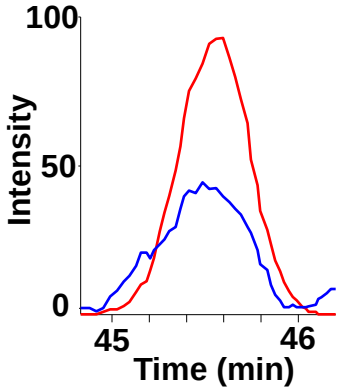

Heavy
Area: 1821432
Intensity: 65273

Light
Area: 997178
Intensity: 30560

C. EGFR pY1197 – Heavy:Control, Light:shTBK1

Figure S8

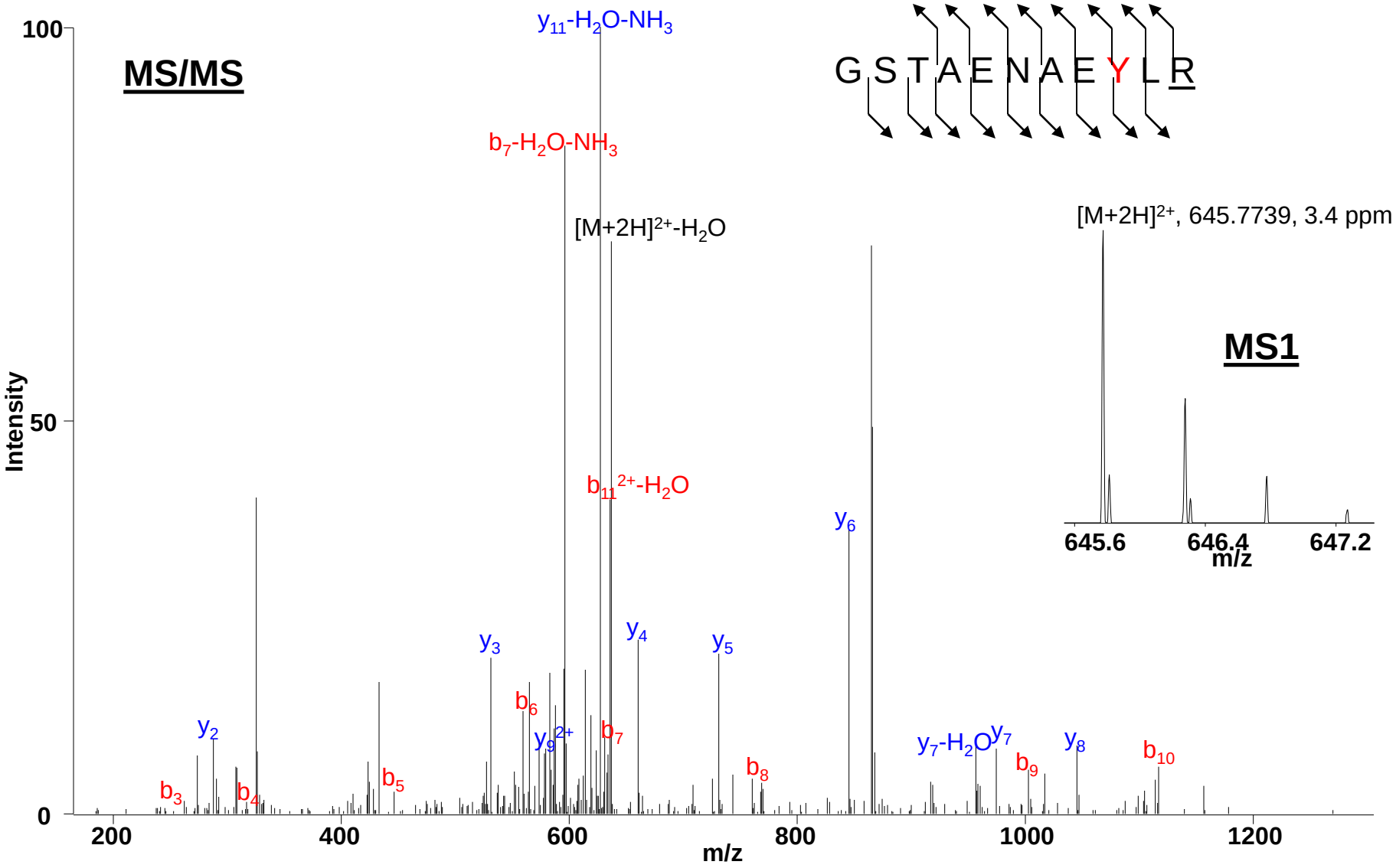

Figure S8

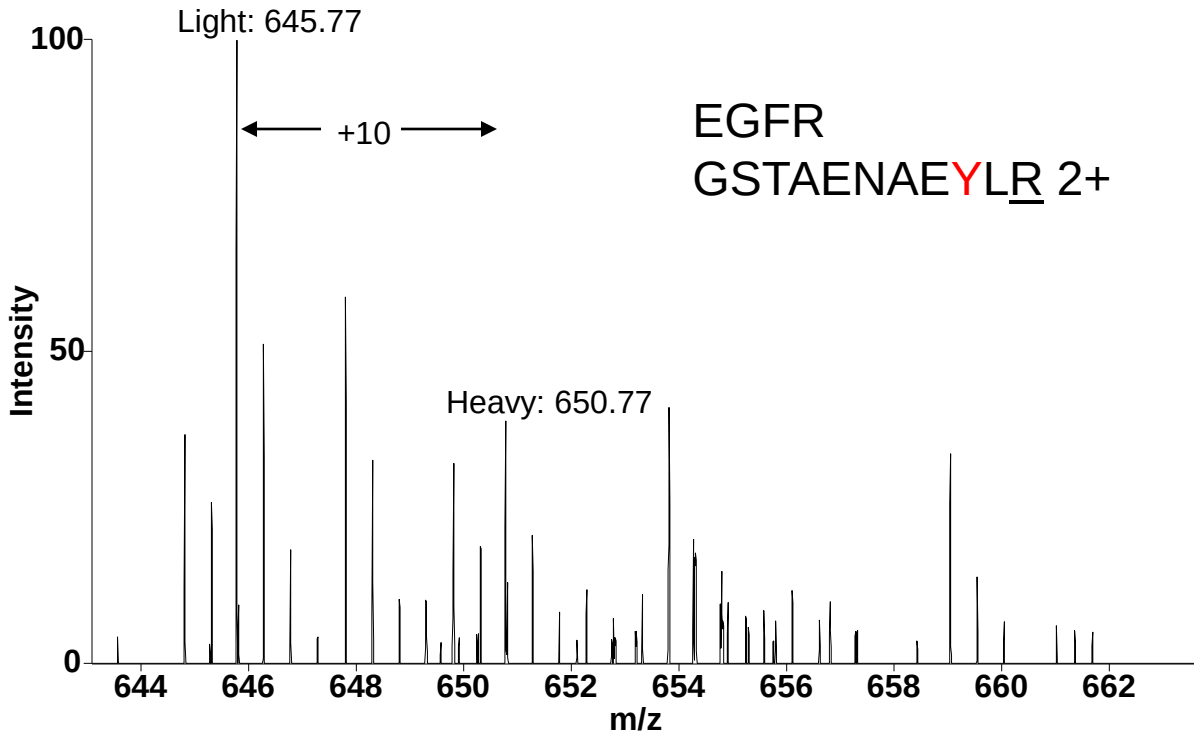
Light: 645.77
+10
EGFR
GSTAENAEYLR 2+
Heavy: 650.77
Intensity
100
50
0
644
646
648
650
652
654
656
658
660
662
m/z

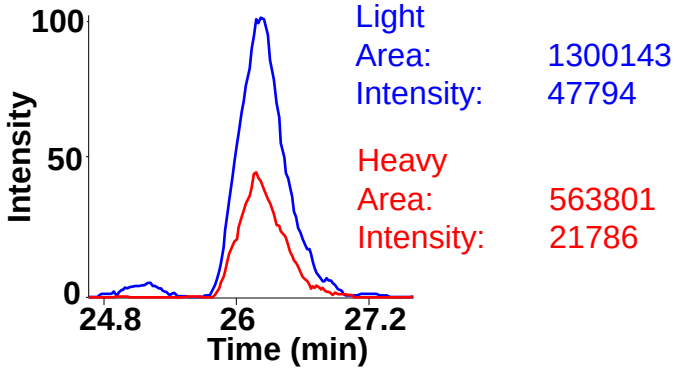
Intensity
100
50
0
24.8
26
27.2
Time (min)
Light
Area: 1300143
Intensity: 47794
Heavy
Area: 563801
Intensity: 21786

D. MAPK3/ERK1 pY204 – Light:Control, Heavy:shTBK1

Figure S8

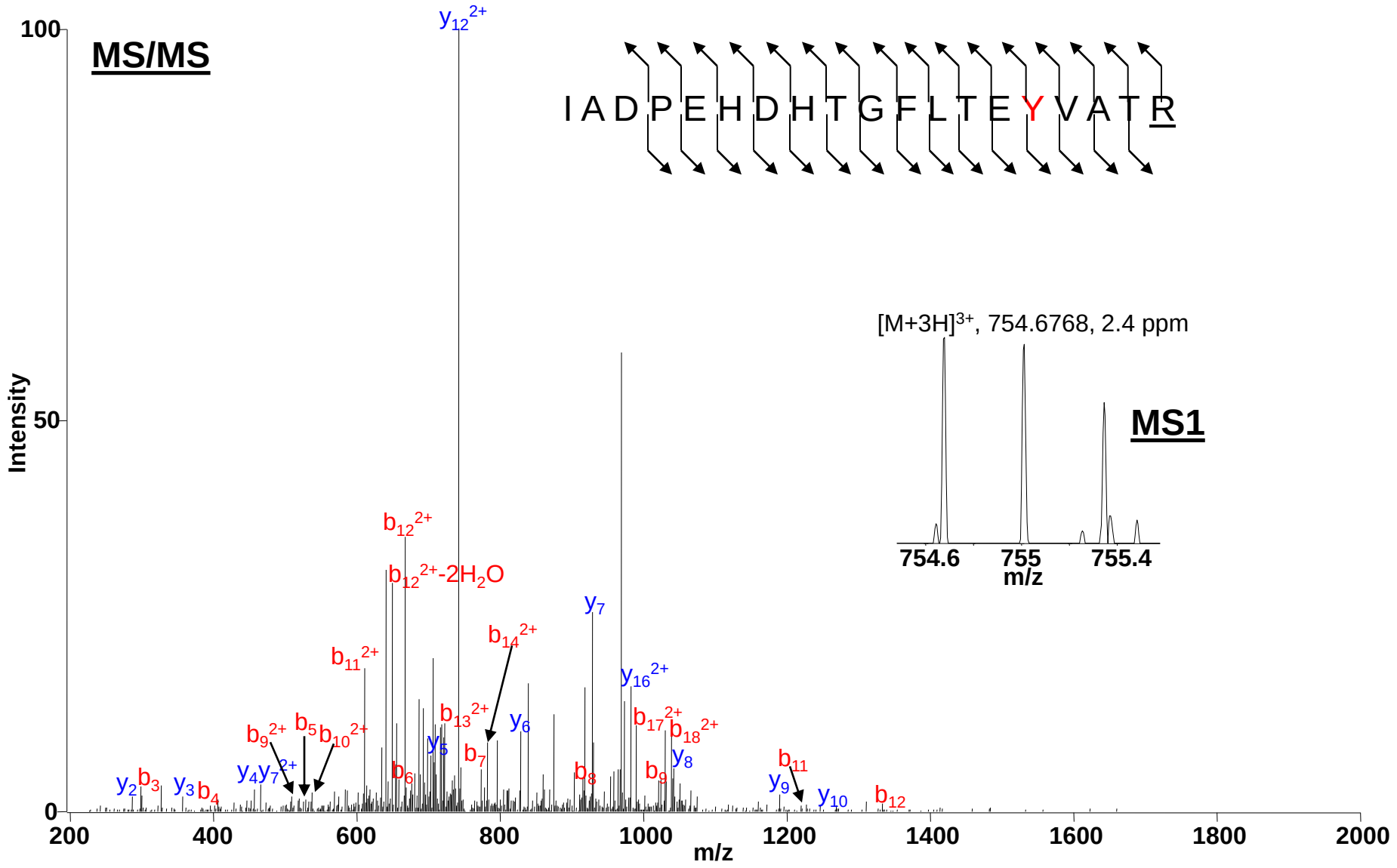

Figure S8

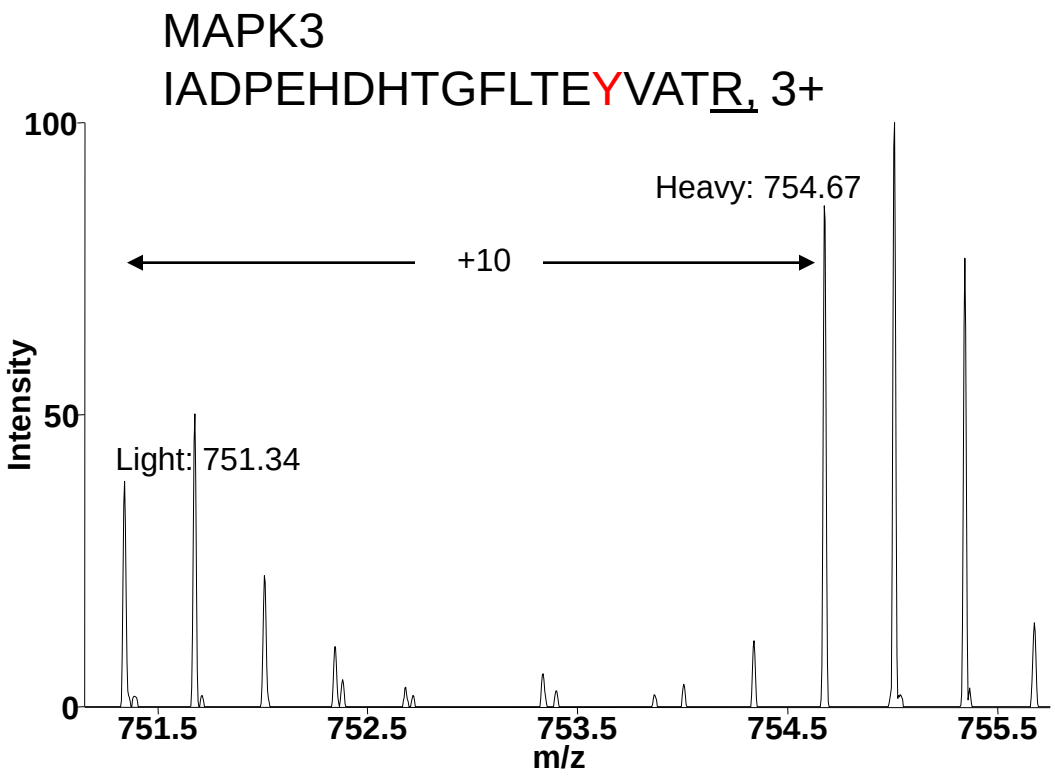

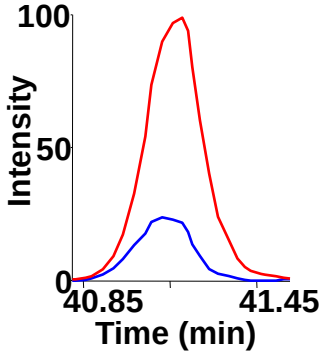

Light
Area: 859729
Intensity: 59338

Heavy
Area: 3582725
Intensity: 247619

E. MAPK1/ERK2 pY187 – Light:Control, Heavy:shTBK1

Figure S8

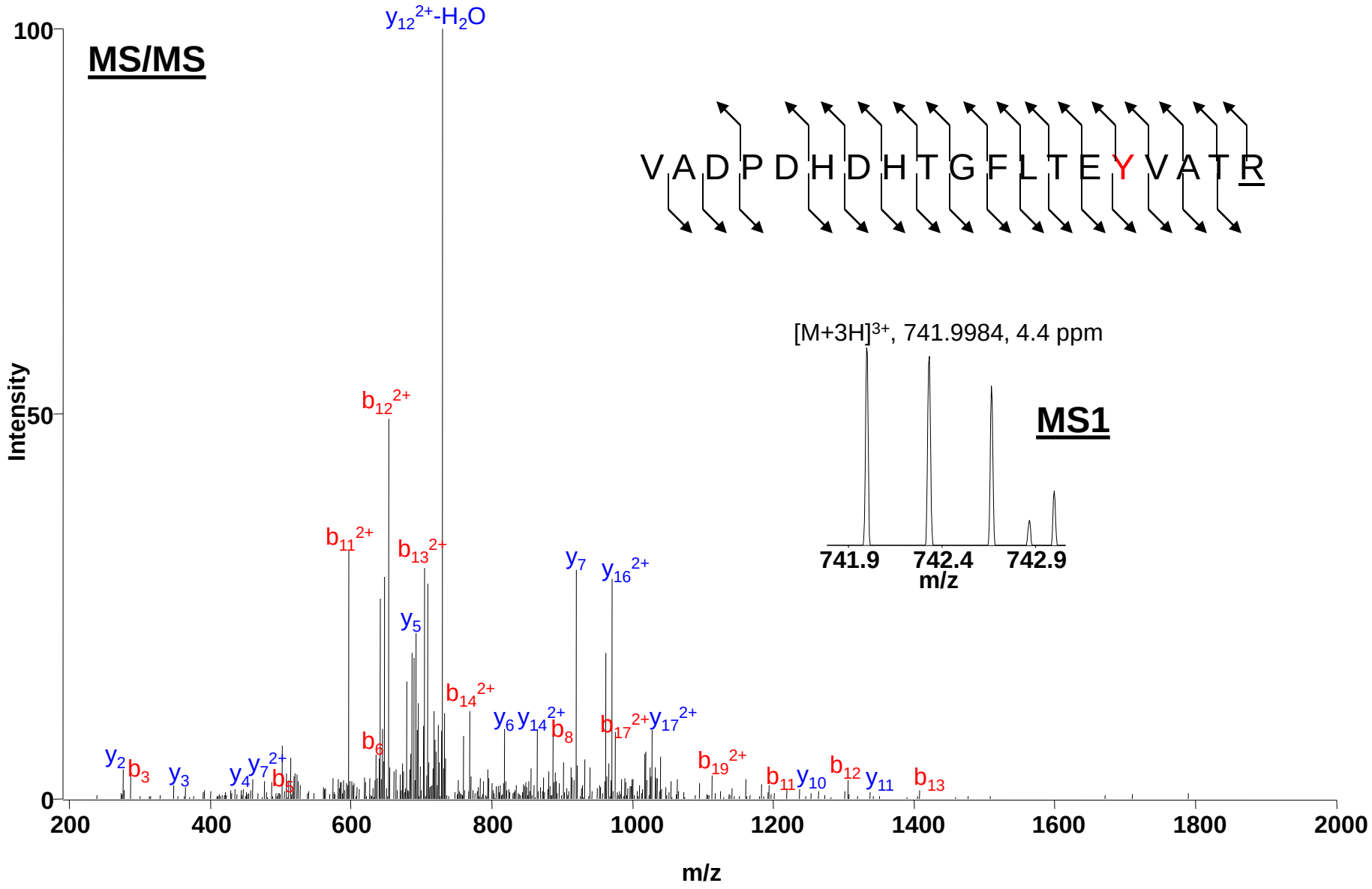

Figure S8

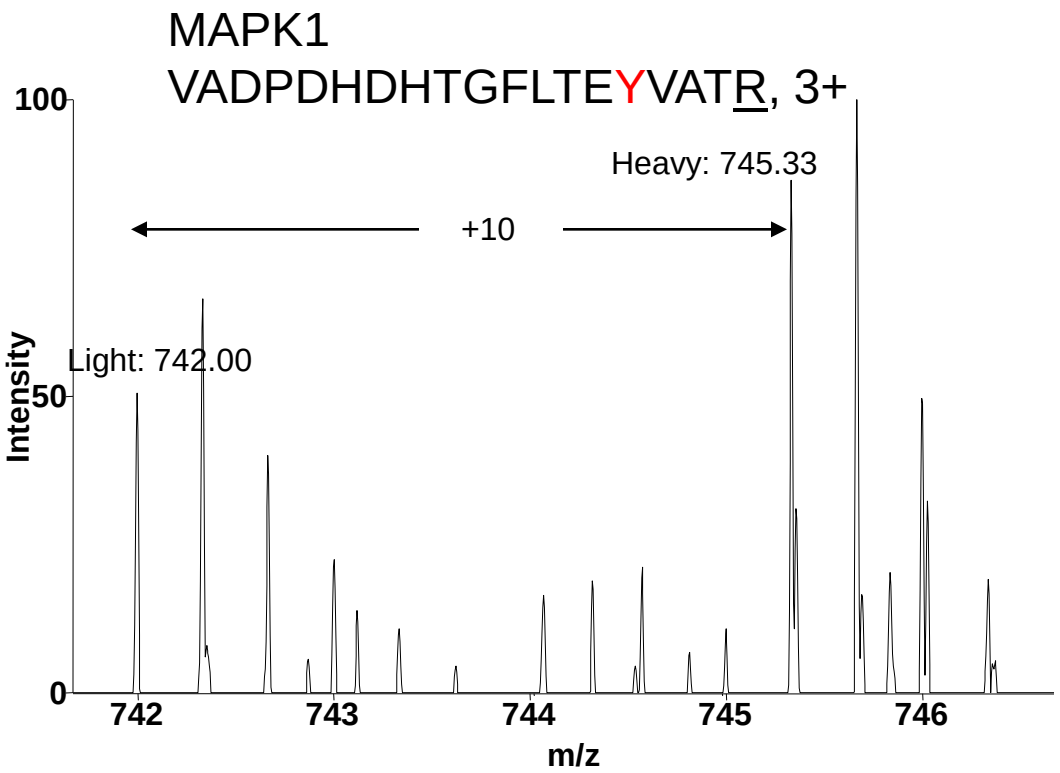

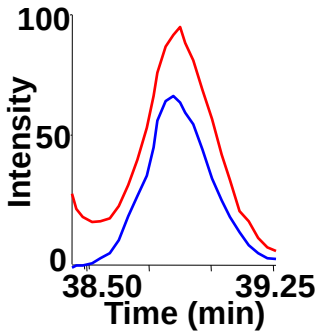

Light
Area: 665363
Intensity: 34580

Heavy
Area: 984618
Intensity: 47114

F. p70/S6K pS424 – Light: Control, Heavy: shTBK1

Figure S8

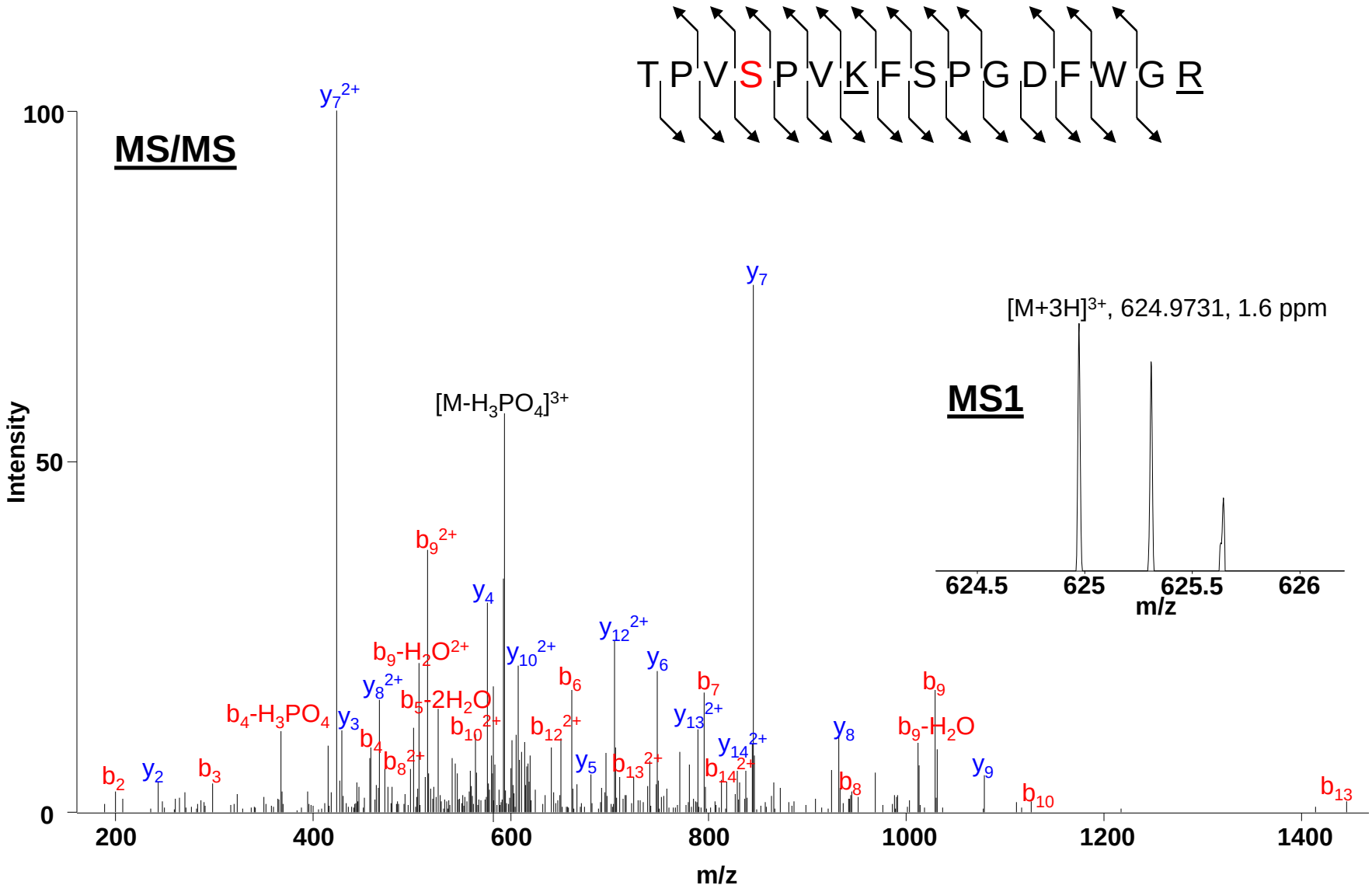

Figure S8

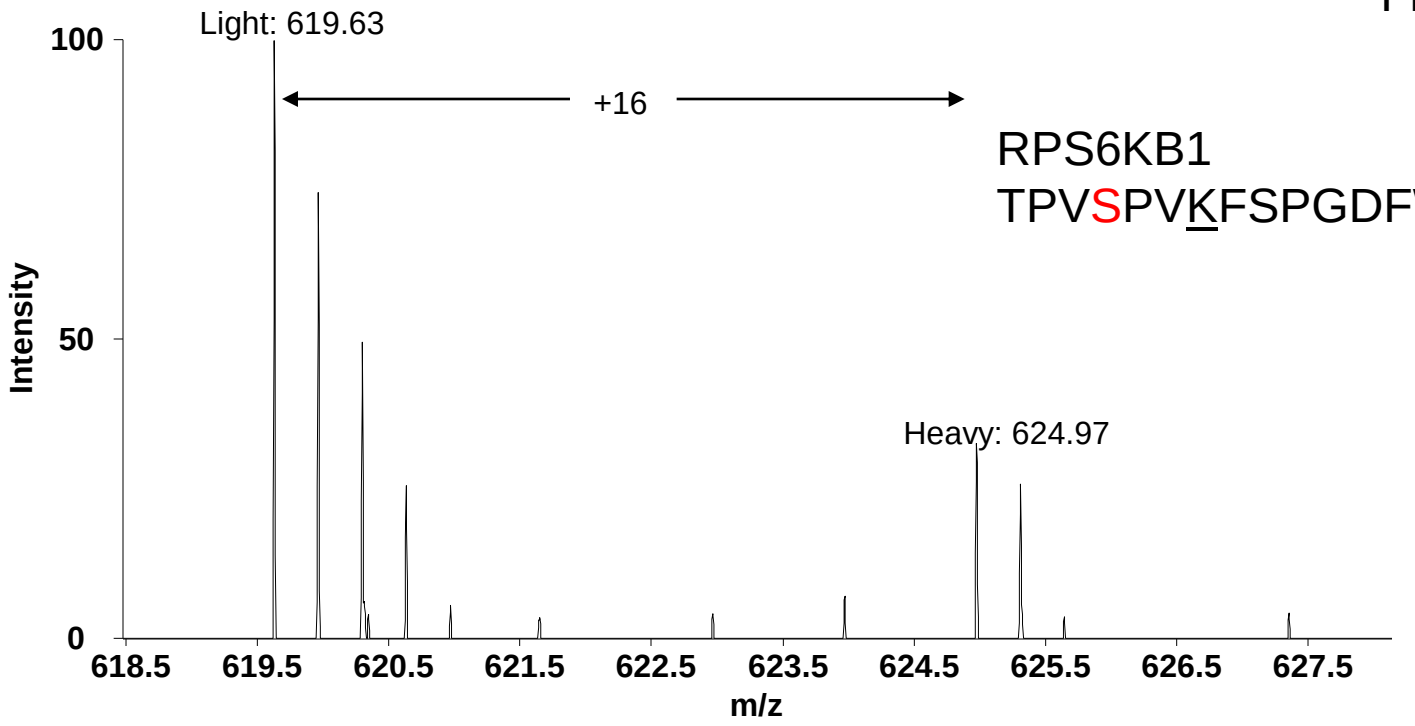

RPS6KB1
TPVSPVKFSPGDFWGR, 3+

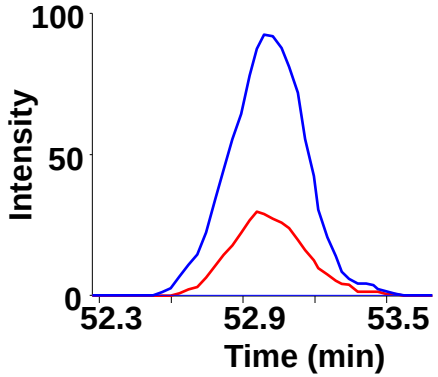

Light	
Area:	2115104
Intensity:	92558
Heavy	
Area:	667042
Intensity:	29937

G. PLK1 pT210 – Light: Control, Heavy: shTBK1

Figure S8

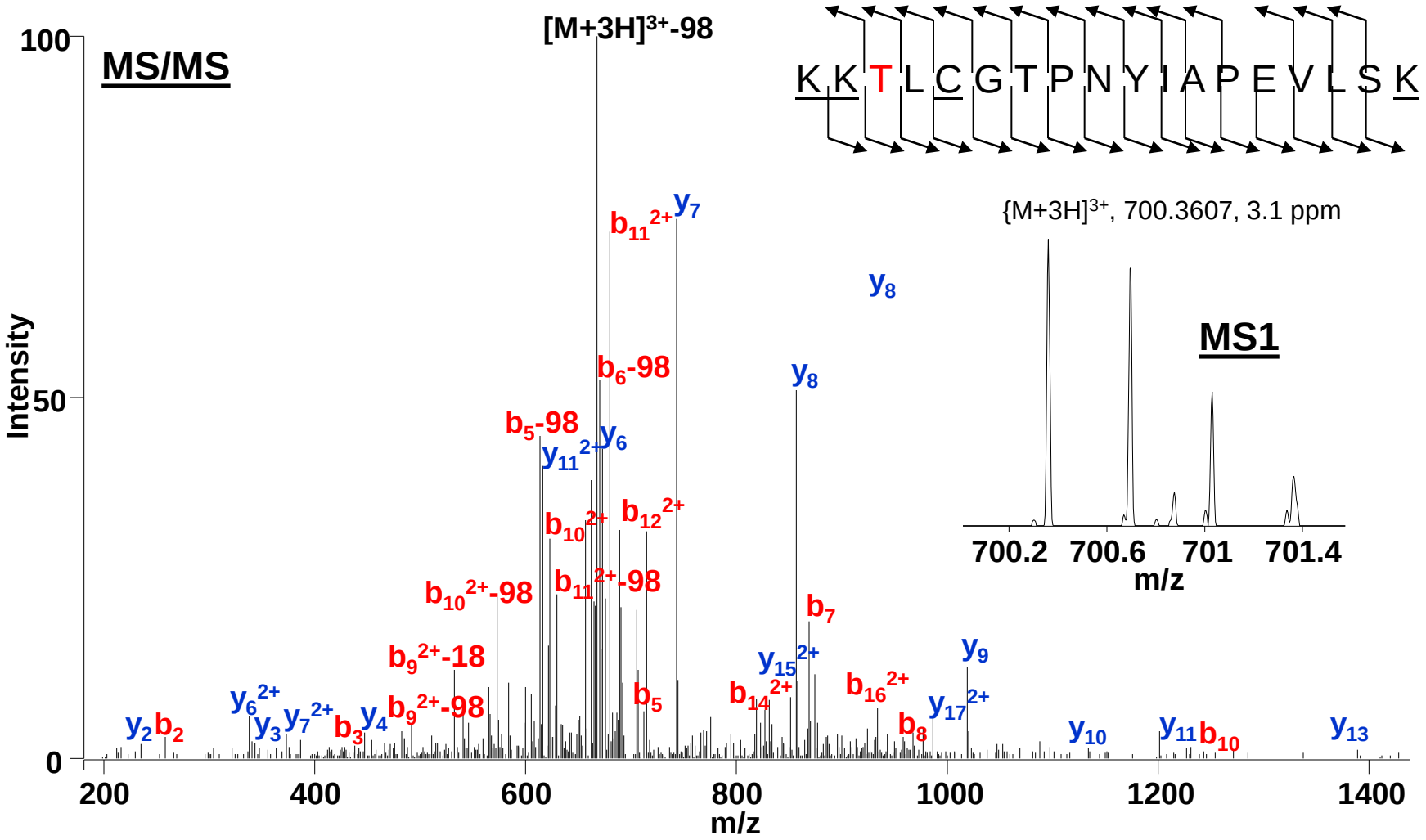

Figure S8

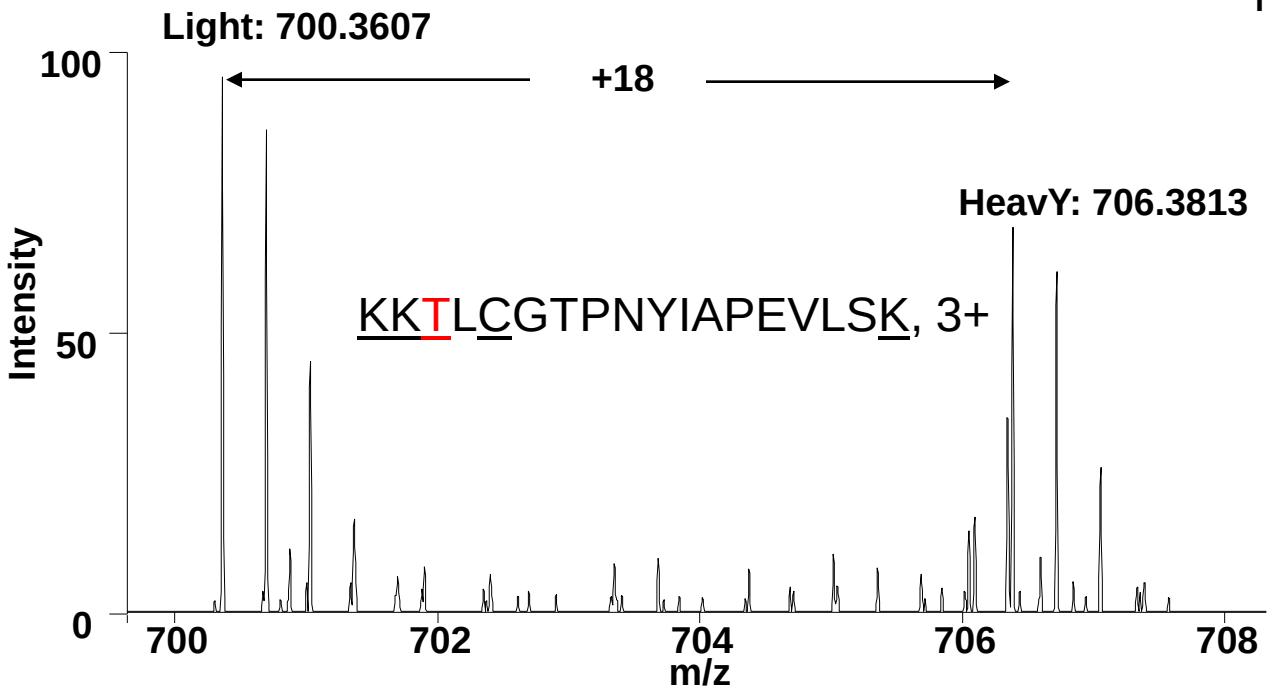

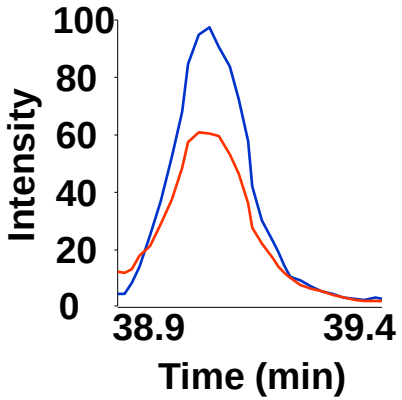

Light
Area: 3084024
Intensity: 189808

Heavy
Area: 2093870
Intensity: 130449

H. Metadherin pS568 – Light: Control, Heavy : shTBK1

Figure S8

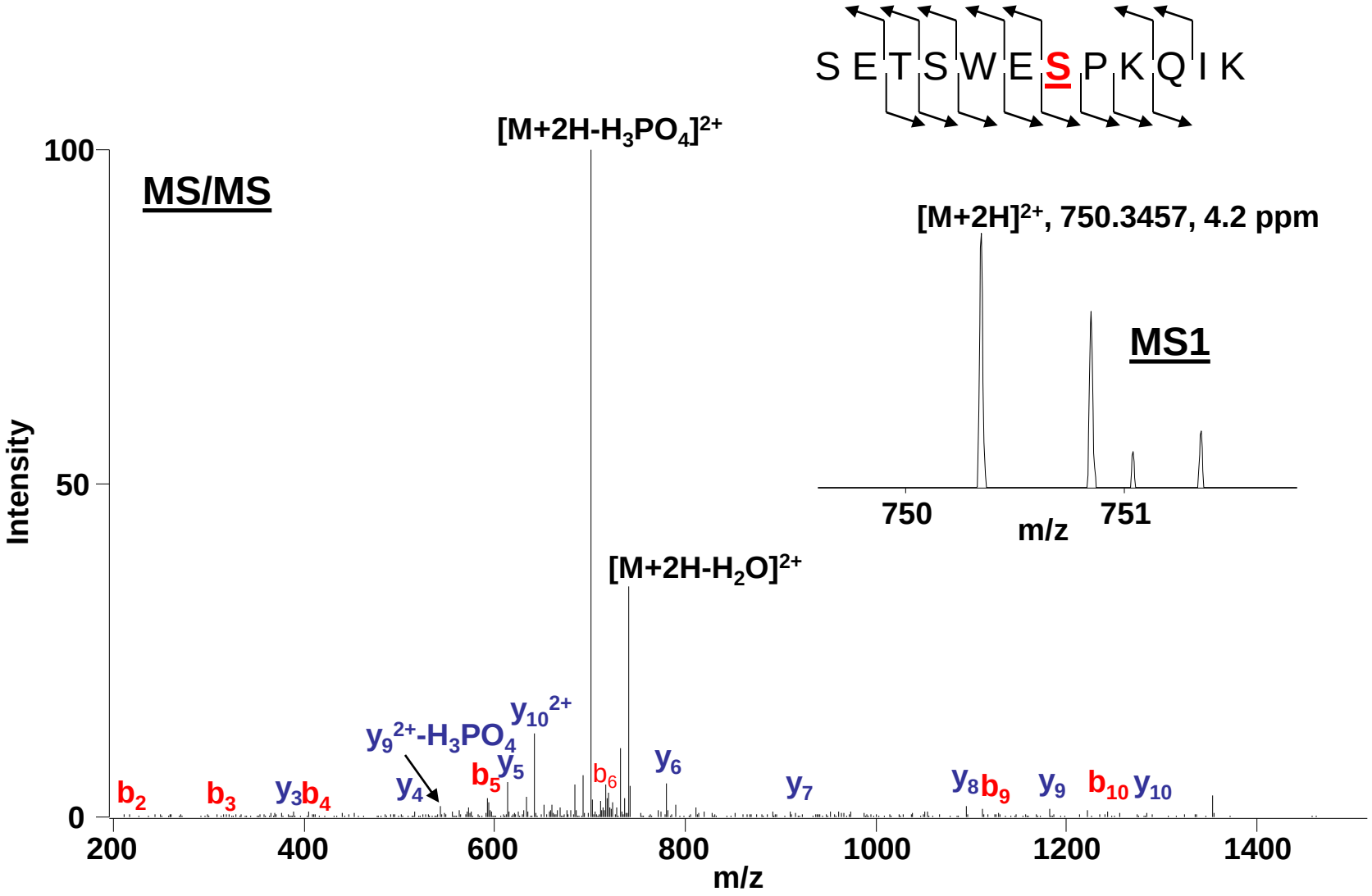

Figure S8

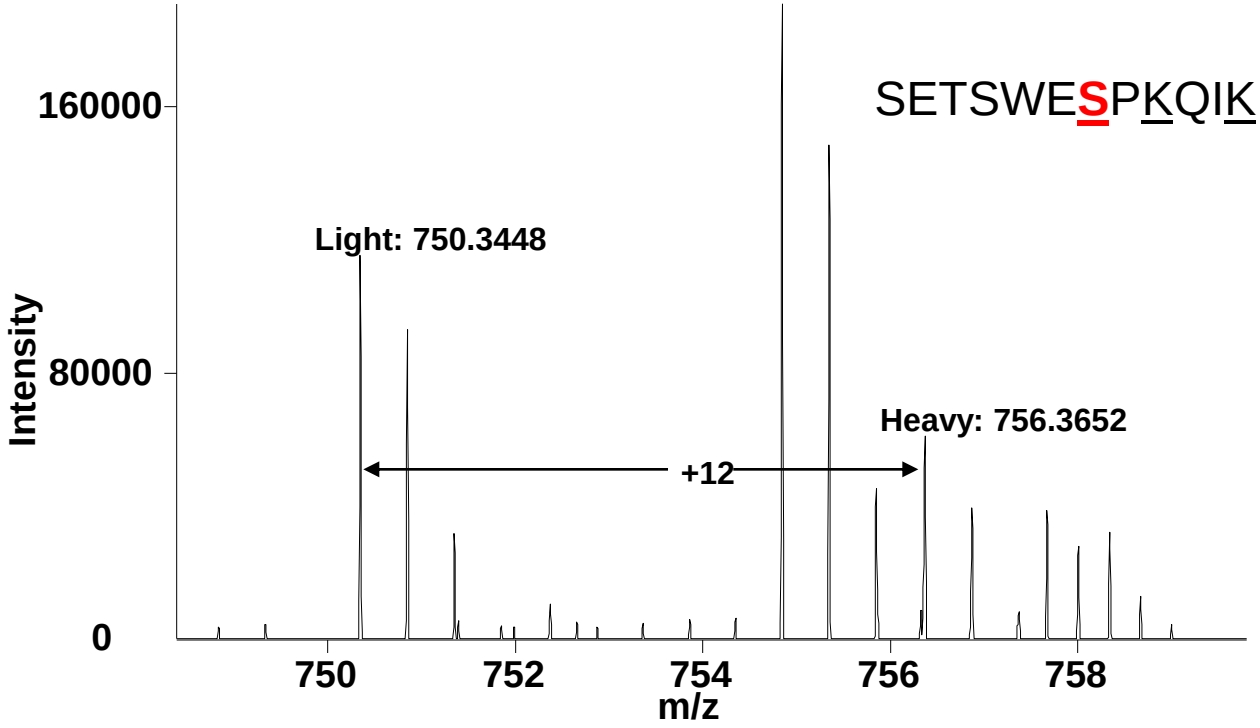

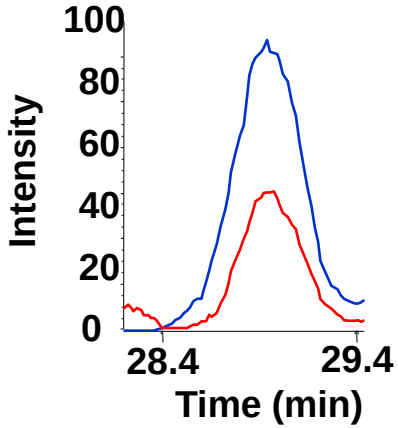

Light
Area: 3725629
Intensity: 148453

Heavy
Area: 1530256
Intensity: 66193

Figure S9

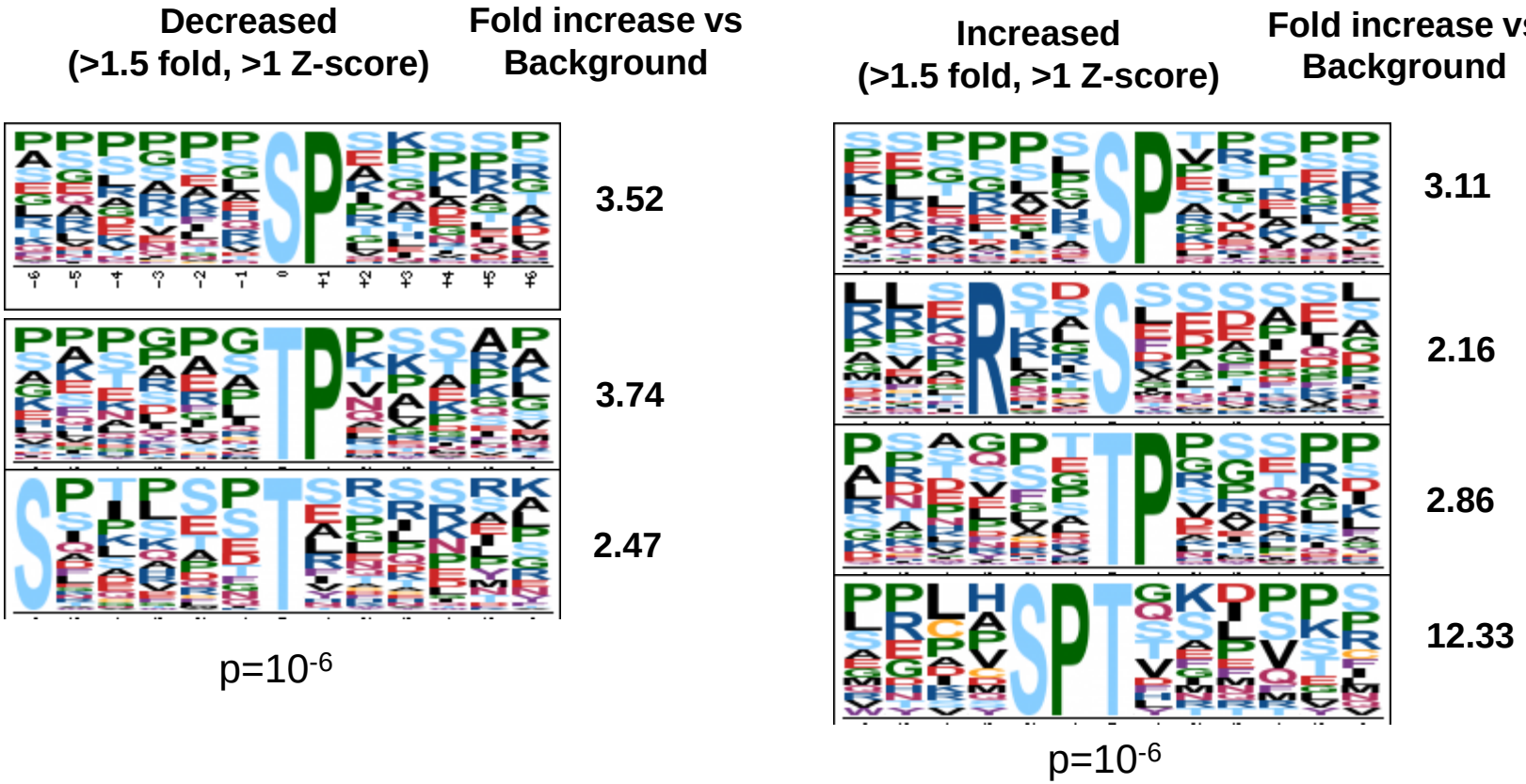
Decreased
(>1.5 fold, >1 Z-score)
Fold increase vs
Background
3.52
3.74
2.47
p=10-6
Increased
(>1.5 fold, >1 Z-score)
Fold increase vs
Background
3.11
2.16
2.86
12.33
p=10-6
Proline-directed
Basophilic

Figure S10

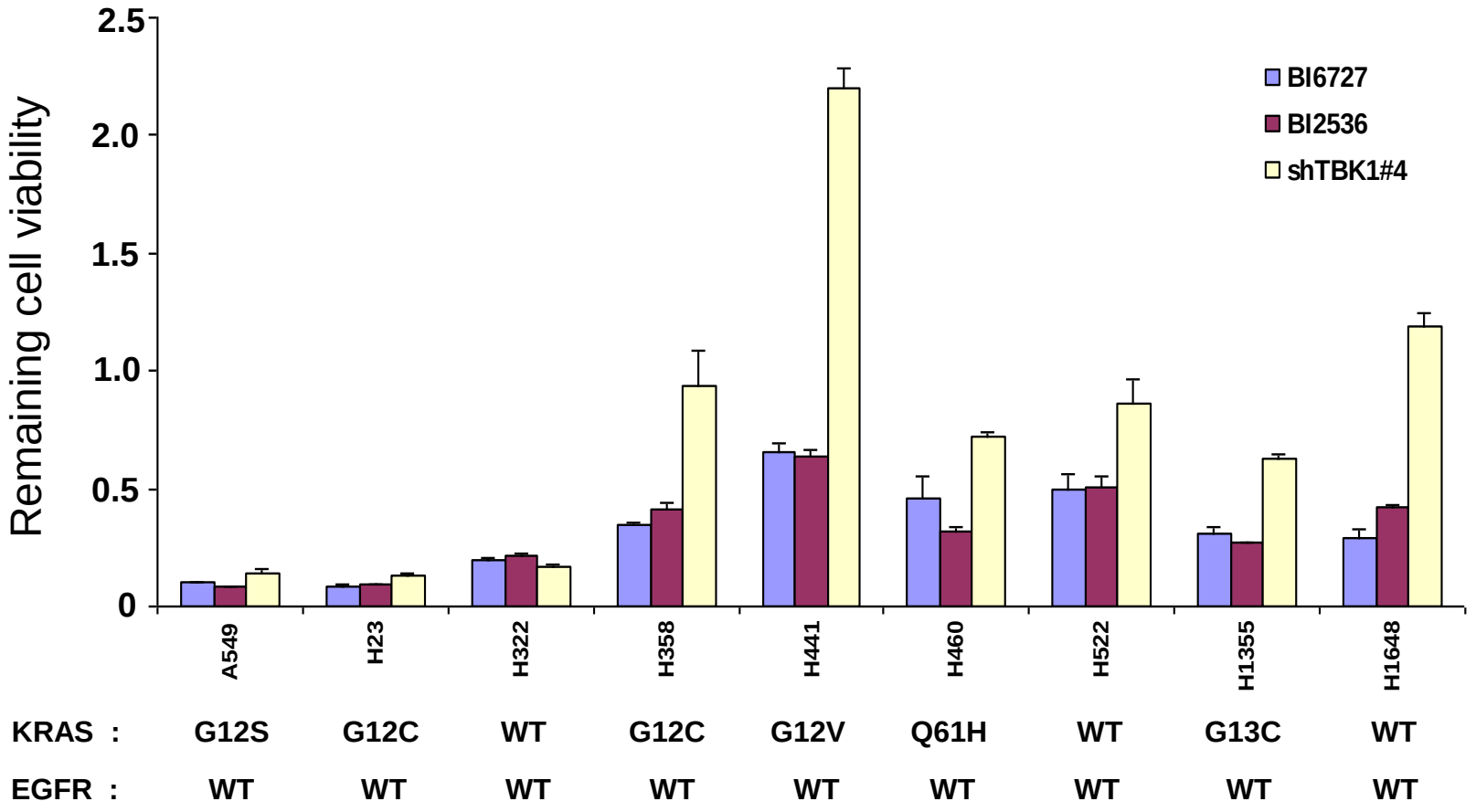
Remaining cell viability
2.5
2.0
1.5
1.0
0.5
0
BI6727
BI2536
shTBK1#4
A549
H23
H322
H358
H441
H460
H522
H1355
H1648
KRAS : G12S G12C WT G12C G12V Q61H WT G13C WT
EGFR : WT WT WT WT WT WT WT WT WT

Figure S11

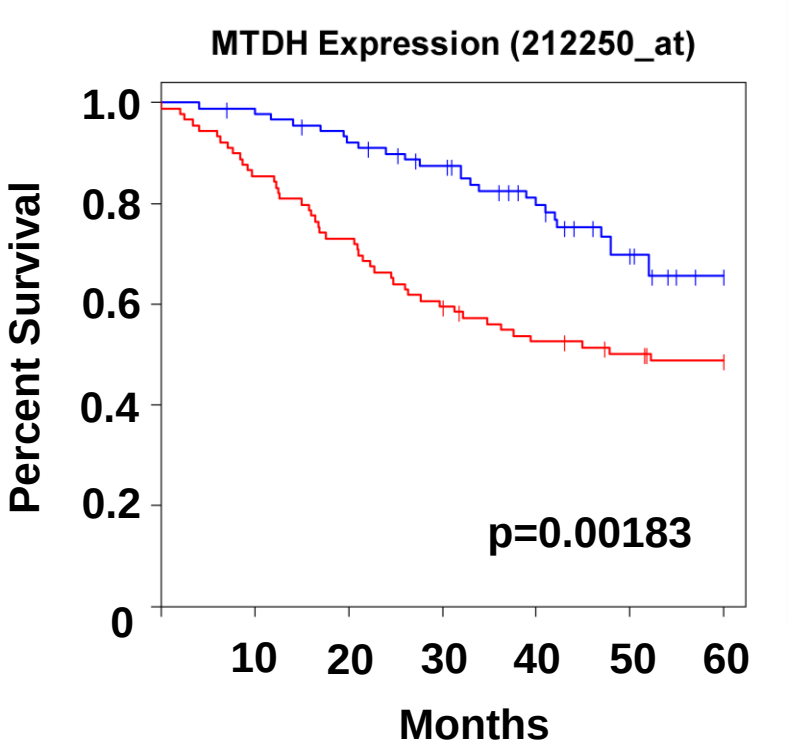
MTDH Expression (212250_at)
Percent Survival
1.0
0.8
0.6
0.4
0.2
0
10
20
30
40
50
60
Months
p=0.00183

Figure S12

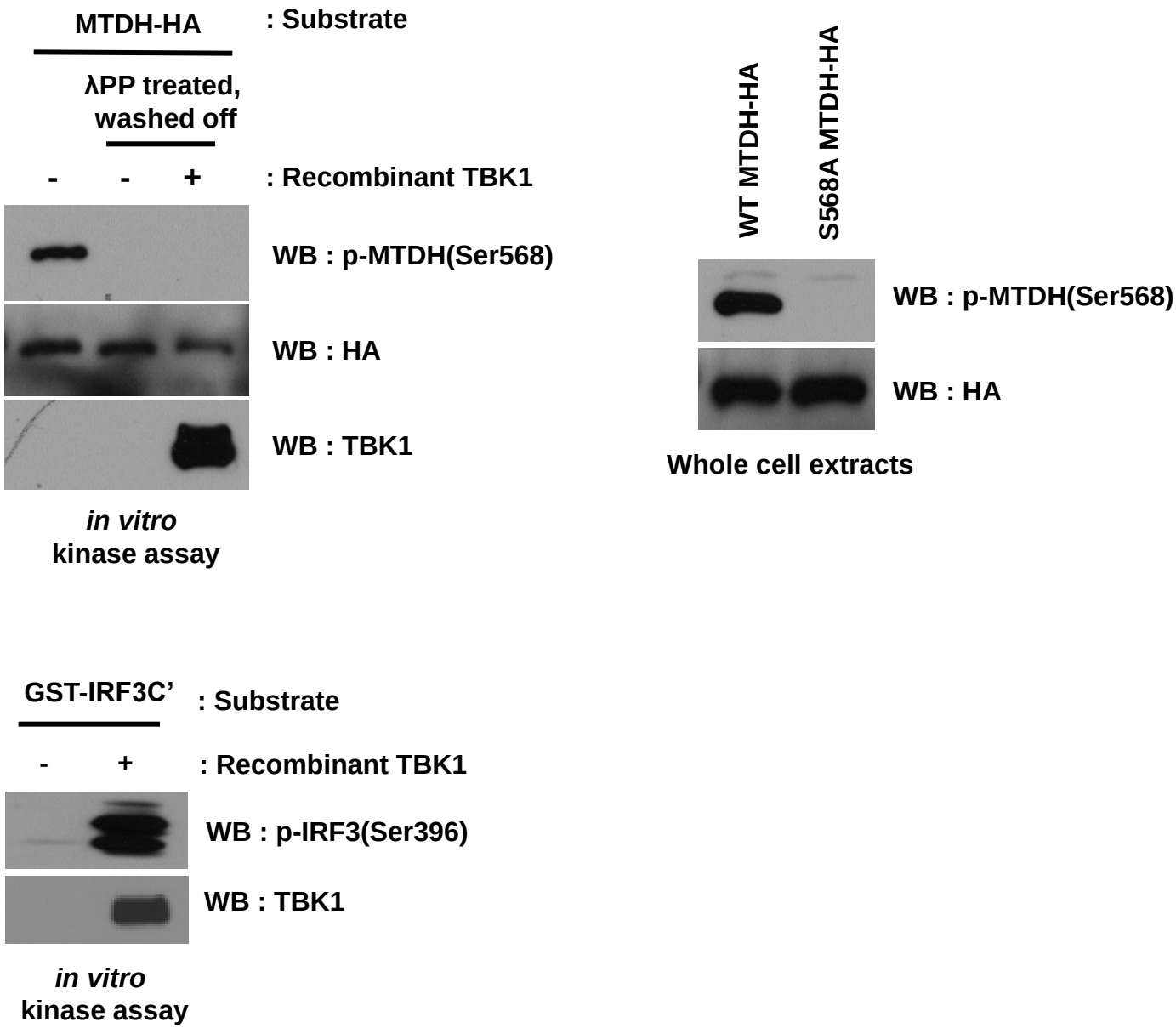
MTDH-HA
: Substrate
λPP treated, washed off
- - +
: Recombinant TBK1
WB : p-MTDH(Ser568)
WB : HA
WB : TBK1
in vitro kinase assay
WT MTDH-HA
S568A MTDH-HA
WB : p-MTDH(Ser568)
WB : HA
Whole cell extracts
GST-IRF3C'
: Substrate
- +
: Recombinant TBK1
WB : p-IRF3(Ser396)
WB : TBK1
in vitro kinase assay

Figure S13

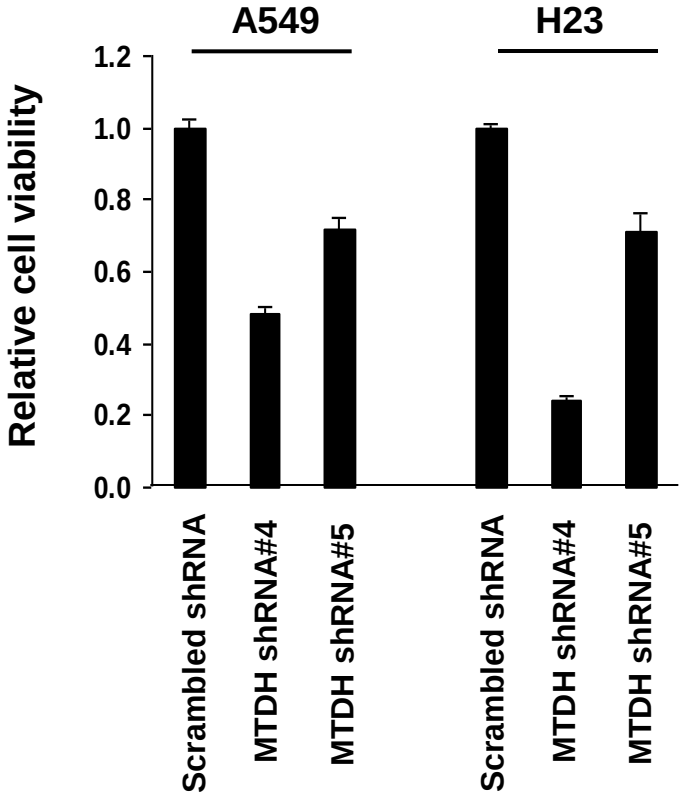
A549
H23
Relative cell viability
1.2
1.0
0.8
0.6
0.4
0.2
0.0
Scrambled shRNA
MTDH shRNA#4
MTDH shRNA#5
Scrambled shRNA
MTDH shRNA#4
MTDH shRNA#5

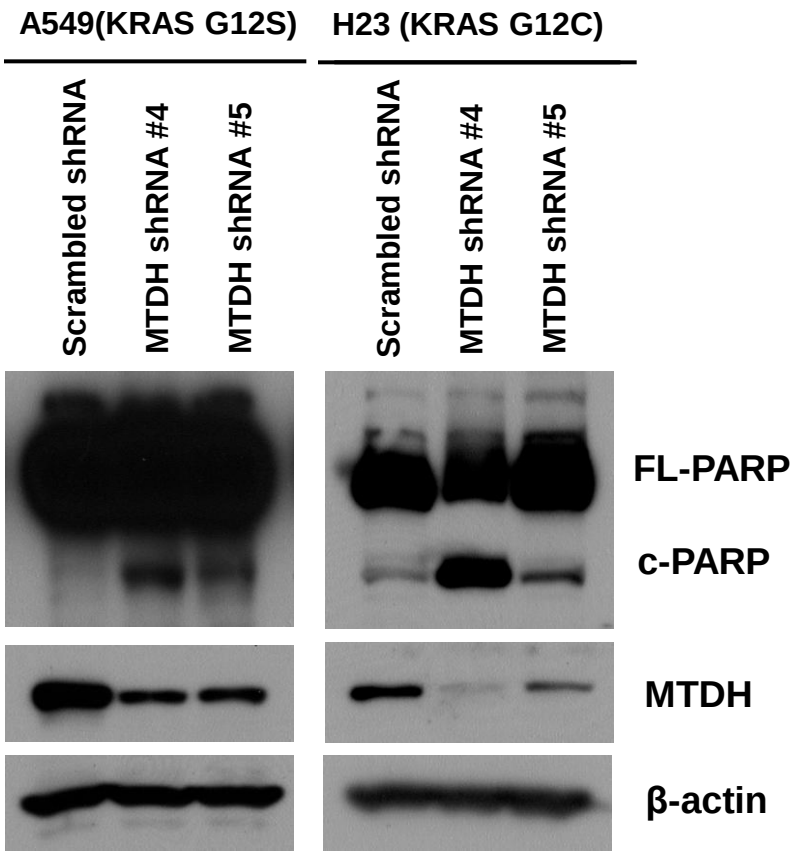
A549(KRAS G12S)
H23 (KRAS G12C)
Scrambled shRNA
MTDH shRNA #4
MTDH shRNA #5
Scrambled shRNA
MTDH shRNA #4
MTDH shRNA #5
FL-PARP
c-PARP
MTDH
β-actin

Figure S14

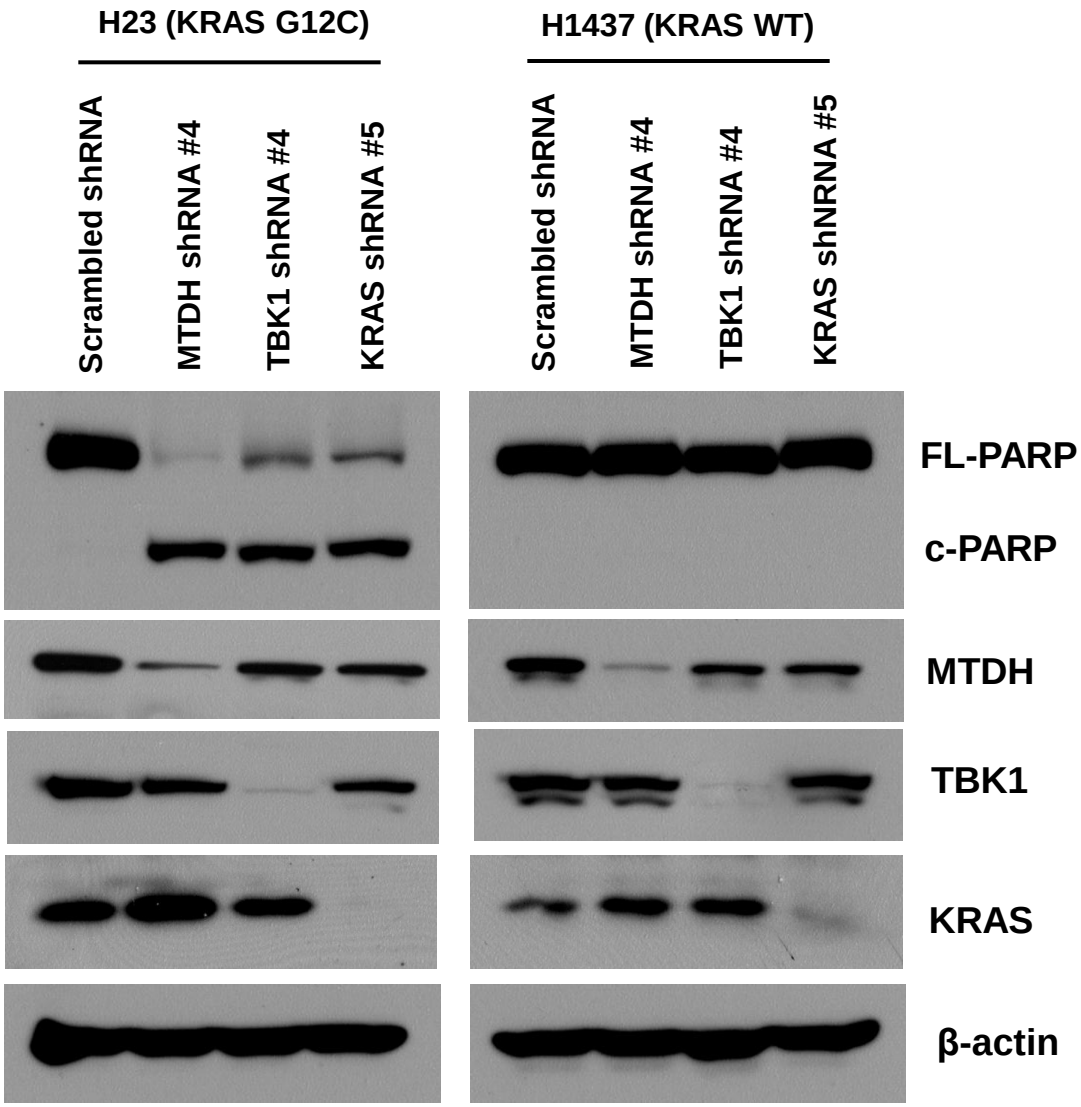
H23 (KRAS G12C)
H1437 (KRAS WT)
Scrambled shRNA
MTDH shRNA #4
TBK1 shRNA #4
KRAS shRNA #5
Scrambled shRNA
MTDH shRNA #4
TBK1 shRNA #4
KRAS shNRNA #5
FL-PARP
c-PARP
MTDH
TBK1
KRAS
β-actin

Figure S15

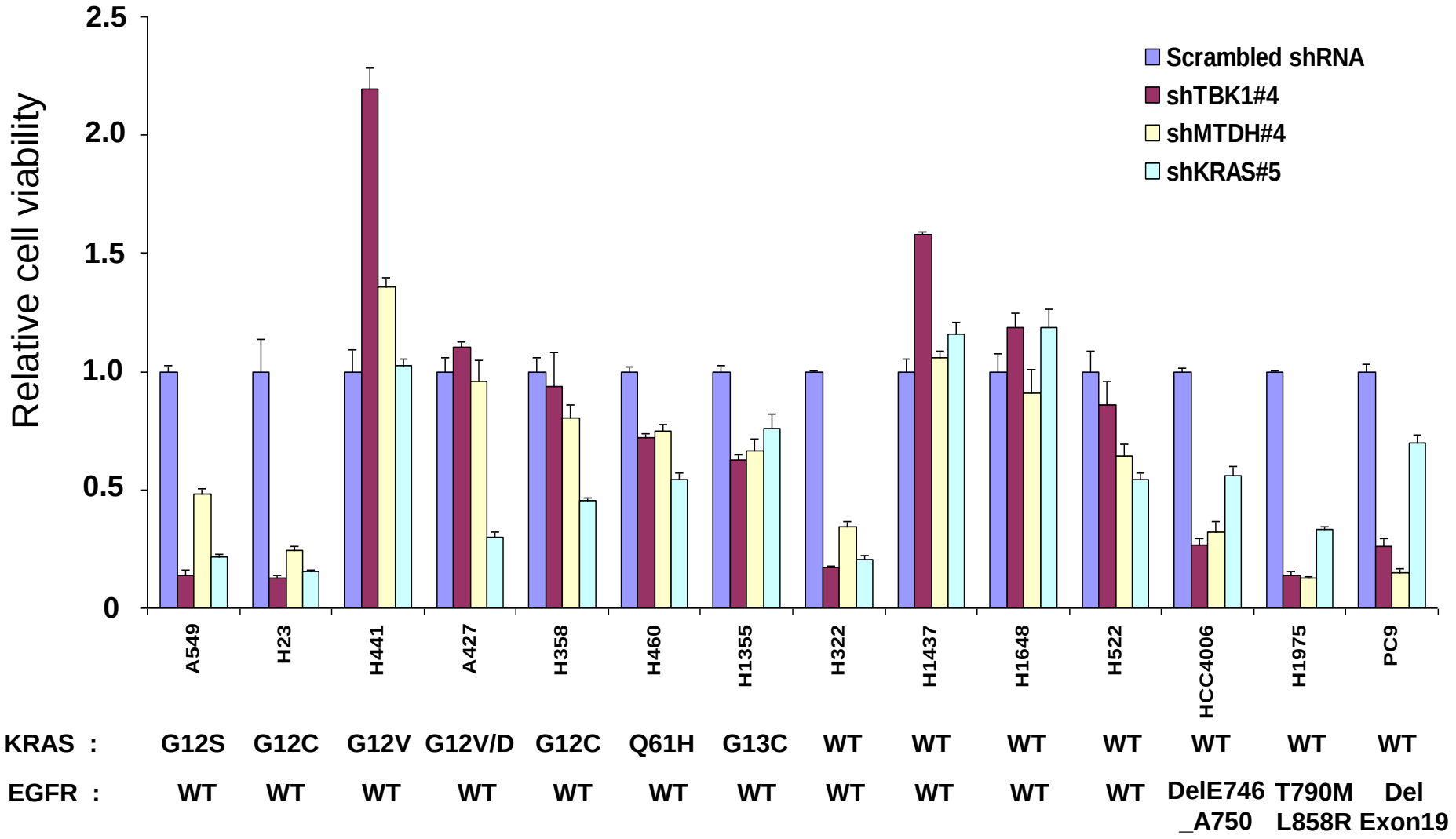
Relative cell viability
2.5
2.0
1.5
1.0
0.5
0
Scrambled shRNA
shTBK1#4
shMTDH#4
shKRAS#5
A549
H23
H441
A427
H358
H460
H1355
H322
H1437
H1648
H522
HCC4006
H1975
PC9
KRAS :
G12S
G12C
G12V
G12V/D
G12C
Q61H
G13C
WT
WT
WT
WT
WT
WT
WT
EGFR :
WT
WT
WT
WT
WT
WT
WT
WT
WT
WT
WT
DelE746_A750
T790M L858R
Del Exon19

Figure S16

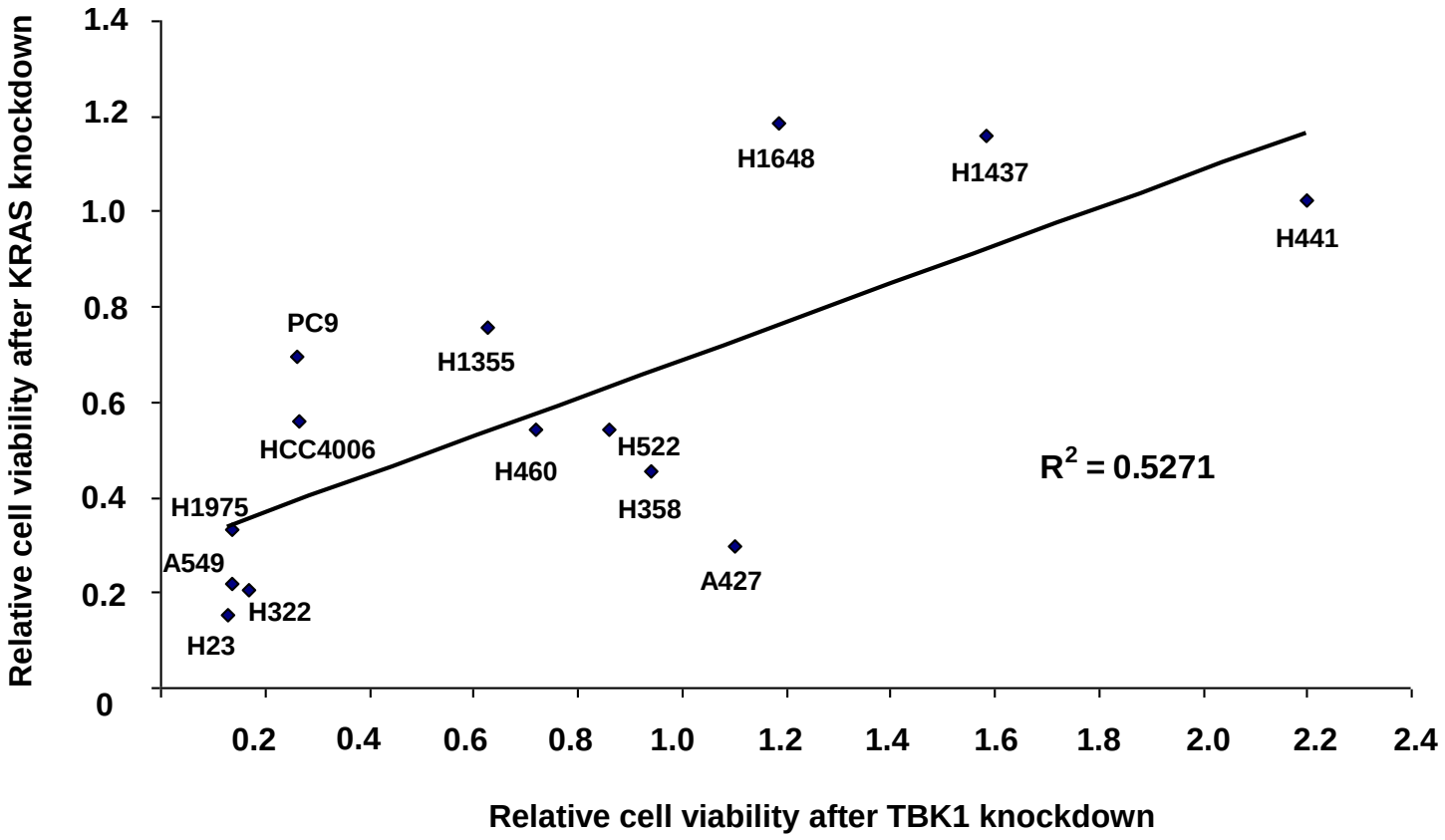
Relative cell viability after KRAS knockdown
Relative cell viability after TBK1 knockdown
1.4
1.2
1.0
0.8
0.6
0.4
0.2
0
0.2
0.4
0.6
0.8
1.0
1.2
1.4
1.6
1.8
2.0
2.2
2.4
H1648
H1437
H441
PC9
H1355
HCC4006
H460
H522
H358
H1975
A549
A427
H322
H23
R2 = 0.5271

Figure S17

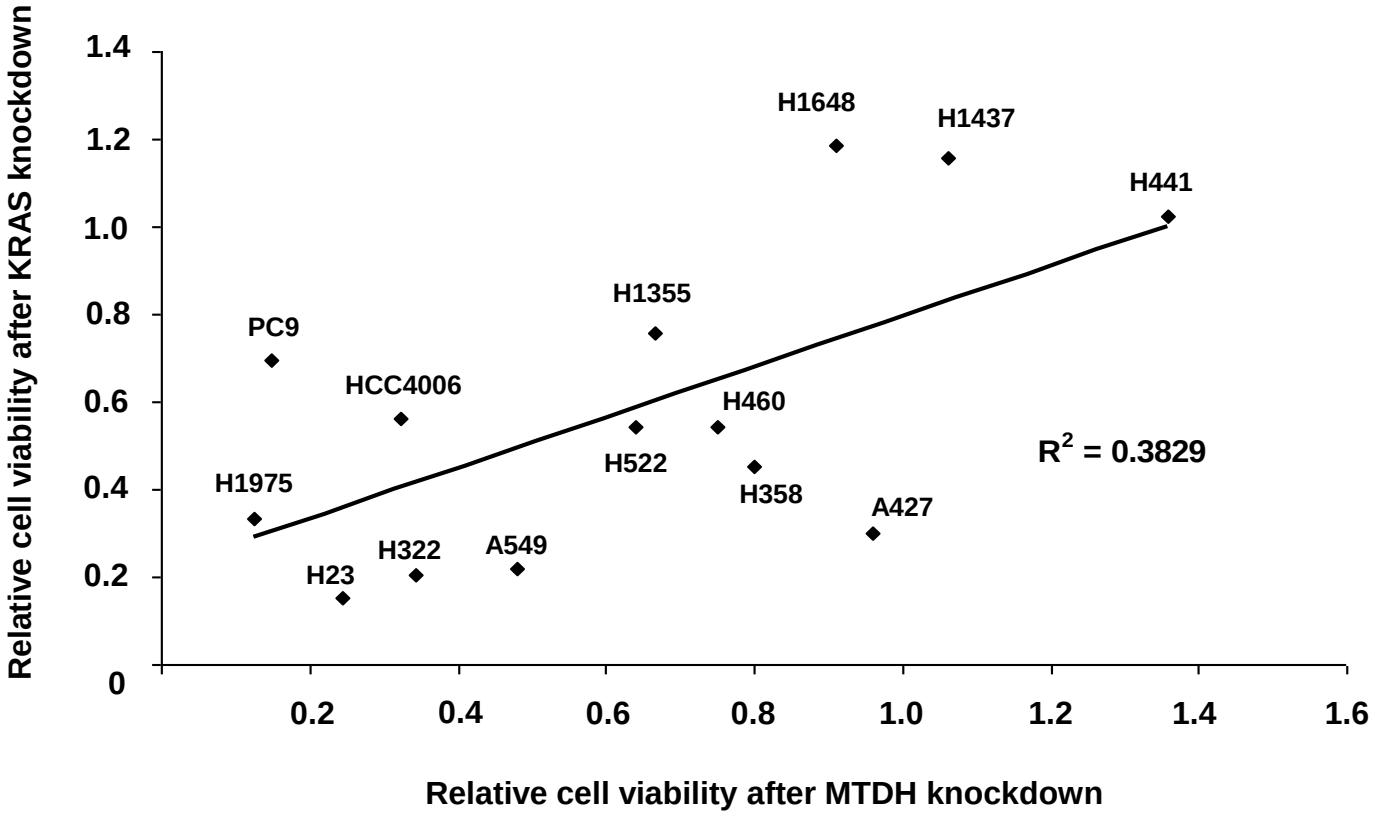
Relative cell viability after KRAS knockdown
1.4
1.2
1.0
0.8
0.6
0.4
0.2
0
0.2
0.4
0.6
0.8
1.0
1.2
1.4
1.6
Relative cell viability after MTDH knockdown
H1648
H1437
H441
H1355
PC9
HCC4006
H460
H522
H358
A427
H1975
H322
A549
H23
R2 = 0.3829

Figure S18

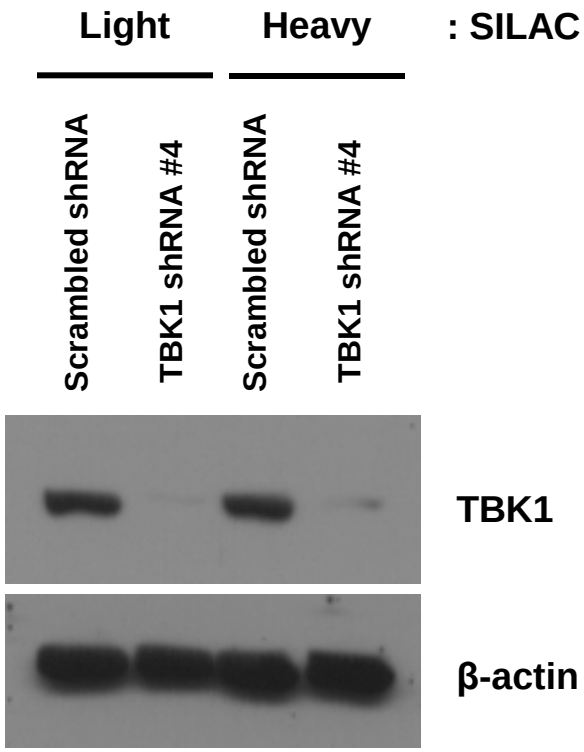
Light
Heavy
: SILAC
Scrambled shRNA
TBK1 shRNA #4
Scrambled shRNA
TBK1 shRNA #4
TBK1
β-actin

Table S1. Pathways Enriched by GeneGO Analysis of TBK1-Regulated Phosphoproteins.	
Down-regulated phosphoproteins (> 1.5 fold, >1 Z-score)	**Up-regulated phosphoproteins (>1.5 fold, >1 Z-score)**
Receptor-mediated HIF regulation	TGF, WNT, and cytoskeletal remodeling
Insulin regulation of translation	Gastrin in cell growth and proliferation
IGF-1 receptor signaling	Cytoskeletal remodeling
Activation of PKC via G-Protein coupled receptor	Oncostatin M signaling via MAPK in human cells
Regulation of EIF-4F activity	β-adrenergic receptors transactivation of EGFR
Sin3 and NuRD in transcription regulation	PTEN pathway
Insulin signaling (generic cascades)	TGFβ-dependent induction of EMT via MAPK
Cell cycle (generic schema)	ETV3 affect on CSF1-promoted macrophage differentiation
Chromosome condensation in prometaphase	VEGFR signaling via VEGFR2 (generic cascades)
Influence of Ras and Rho proteins on G1/S transition	IL-15 signaling

Table S2: shRNAs used in this study		
shRNA	**TRC identifier**	**NM number**
shTBK1#1	TRCN0000003182	NM_013254
shTBK1#4	TRCN0000003185	NM_013254
shKRAS#5	TRCN0000033260	NM_033360.2
shMTDH#4	TRCN0000153105	NM_178812
shMTDH#5	TRCN0000151467	NM_178812